令和２年度卒業論文

２成分系流体の熱と質量の交差輸送係数の粒子間ポテンシャル依存性

物理工学科

増渕研究室

学生番号： 081720078

氏名： 大石達真

Abstract

We paid attention to the Soret effects in which the mass flux is induced by the temperature gradient. Soret effect is generally characterized by the cross transport coefficient of the fluid mass and heat. To understand the cross transport coefficient in binary mixture of fluids, we considered a system in which the two-component fluids (particle 1 and particle 2) are in equilibrium. We determined the cross transport coefficient by using the Green-Kubo formula. We focused on how the inter-molecular potentials influence the cross transport coefficients when we vary mass ratio and the potential parameters for LJ and WCA potentials. We found that, when the symmetry of the system is held, the cross transport coefficients is zero. Meanwhile, even for the WCA potential, which solely generates a repulsive force, the cross transport coefficient is not 0 when the symmetry is broken. We found that LJ potential and WCA potential exhibited different behavior due to the attractive force and the attractive force plays an important role for the cross transport coefficient. We also found that in a high temperature, the cross transport coefficient is insensitive to the difference of the interaction potential.

Contents

Chapter 1

Introduction

1.1 What is the Soret effect

Liquids and gases that we see everywhere in our daily life behave differently depending on the temperature and pressure. Physical properties of materials under equilibrium at uniform temperature and pressure have been widely studied. However, despite the fact that the temperature of the environment, in which we usually live is non-uniform, physical properties under such conditions are not fully elucidated. Thus if we could theoretically understand the physical properties of substances under temperature gradients in this way, it would be a highly rippled knowledge that would support the development of various science and technology, and product management.

Among the physical properties under the temperature gradient, let us pay particular attention to the Soret effect[1]. The Soret effect is an effect, in which for a binary mixture of fluids, a mass flux is induced by a temperature gradient. The Soret effect is described by a parameter so called the Soret coefficient (transport coefficient), which describes the mass transfer under the temperature gradient. The phenomenological equation of material flux $\boldsymbol{J}$ due to the thermal diffusion under the temperature gradient is written as follows using the diffusion coefficient(D) and the thermal diffusion coefficient(D_T).

$$\boldsymbol{J} = D\frac{\partial c}{\partial x} + D_T\frac{\partial T}{\partial x}, \tag{1.1}$$

where we define the concentration of one of the fluids c, the direction of the temperature gradient x and temperature T. In the steady state,flux J is 0 and the Soret coefficient is defined as $S_T = \frac{D_T}{D}$ and satisfy

$$S_T = -\frac{\partial c}{\partial x}/\frac{\partial T}{\partial x}. \tag{1.2}$$

The fluid moves to the cold side when S_T is positive, whereas it moves to the hot side when S_T is negative.

1.2 Previous researches

The Soret coefficient in a sufficiently dilute gas has been quantitatively described by Chapman and Enskog[2][3] according to the theory of rigid body collisions. However, for the case of liquids, the collisions are complicatedly correlated, and it becomes difficult to determine the Soret coefficient theoretically [4].

To determine the Soret coefficient in liquids, various experiments have been performed. When we consider the mass dependence, analogous results to dilute gas are observed for some liquid mixtures for which the heavier particles have a positive Soret coefficient , even the polymer solutions. However, in a few cases, the heavier particles have negative Soret coefficient values. For example, Giglio and Vendramini[5] reported that a negative Soret coefficient for a polymer dissolved in water and Kita[6] reported that the Soret coefficient of water in various aqueous solutions changes its sign depending on the water fraction due to the influence of hydrogen bonds. This phenomenon hardly be analyzed because we have difficulties to reproduce the inter-molecular potential of water.[7]. Indeed, in the simulation studies, the researchers performed simulations by using various models of water to reproduce the experiments.[8, 9, 10]. They reproduced the sign change of Soret coefficients depending on the water fraction, whereas they cannot explain the behavior of water theoretically.

To understand the Soret coefficient in liquid. Various studies have been conducted on the Soret coefficient of liquids from simple systems.[11, 12, 13, 14] For example, Vogelsang[13, 15] et al. used the well-known Lennard-Jones (LJ) potential to calculate the Soret coefficient for interacting systems. They discussed the mass dependence and potential parameter dependence on the Soret coefficient, although they can not perform detailed analysis on how the potential (LJ potential) influences the Soret coefficient. It is very important to consider complicated interactions like hydrogen bonds and electron attractions. However, at present, the theoretical analysis of the Soret coefficient is not fully accomplished even for simple system that excludes complicated potentials.

In this study, we focus on how the inter-molecular potentials influence Soret coefficients when we change mass ratio and potential parameters in a simple systems. We performed molecular dynamics simulations of binary systems containing two different monoatomic fluid particles. The particles interact with each other via LJ and WCA potentials. Under equilibrium states, we observed the particle motion to obtain the Soret coefficient. We discuss what determines the Soret coefficient using the basic LJ potential and the simpler WCA potential. Moreover, by comparing these potentials, we investigate how the Soret coefficient changes its sign by the attractive interaction.

1.3 Purpose and constitution in this study

The purpose of this study is to clarify the mechanism of the Soret effect in terms of the interparticle potential dependence of the cross-transport coefficient of heat and mass in two-component fluids. This thesis consists of 5 chapters

chapter 1 : We explain the previous researches about the Soret effect and the purpose of this study.

chapter 2 : We explain the system, the simulation methods and derivation of the transport coefficients in the equilibrium state.

chapter 3 : We analyze the transport coefficients when we change the mass, the potential parameter and the temperature.

chapter 4 : We summarize the result of the Soret coefficients in the liquids to consider the effects of the interpartile potentials.

chapter 5 : Appendix

Chapter 2

Model and Simulations

2.1 Summary

In this study, I investigated how the mass and heat cross-transport coefficients in binary fluids changes depending on the potential parameters and the mass contrast using the molecular dynamics method. The simulation of this study was performed by LAMMPS (Large-scale Atomic/Molecular Massively Parallel simulator)

2.2 Model

2.2.1 Introduction

Various studies have been conducted on the Soret coefficient of liquids. However, they have not reached a detailed discussion on what determines the sign of the Soret coefficient and what mechanism lying behind. Therefore, we simulated particles motion in two-component fluids consisting of particle 1 and particle 2 in equilibrium by molecular dynamics. For particle motion in LJ potential and WCA potential, the parameters were systematically changed and the effects were analyzed. Then, we investigated how the attractive interaction affects the transportation coefficient.

2.2.2 Interparticle potential

In this simulation, the interparticle potential is set to LJ potential and WCA potential. The potential acting on the particles of the i component and the particles of the j component is defined as follows.

$$U_{LJ}(r) = \begin{cases} 4\varepsilon_{ij}\left[\left(\frac{\sigma}{r_{ij}}\right)^{12} - \left(\frac{\sigma}{r_{ij}}\right)^{6}\right] & (r_{ij} \leq r_c) \\ 0 & (r_{ij} > r_c) \end{cases} \tag{2.1}$$

σ is the particle size, ε_{ij} is the strength of the interaction between the i component and the j component, and the cutoff length of the LJ potential is ($r_c = 3.0$), WCA potential is $r_c = 2^{1/6}\sigma$.

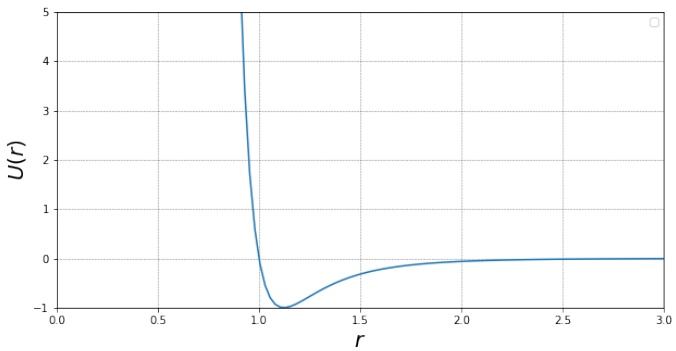

Figure 2.1: LJ potential

2.2.3 Simulation parameter

In this system, units of length, energy, mass, and temperature are chosen as σ, ε_{11}, and mass m, and k_B. The other parameters of the simulation are set as follows according to the chosen units.

various parameter		
m	mass of particles 1	1.0
M	mass of particles 2	1.0
N_1	number of particles 1	16000
N_2	number of particles 2	16000
V	volume	$(35.7561)^3$
ρ	density	0.7
ϕ	number fraction	0.5
σ	size of particles	1.0
ε_{11}	interaction parameter between particle 1	1.0
ε_{22}	interaction parameter between particle 2	1.0
ε_{12}	interaction parameter between particle 1 and 2	1.0
T	temperature	1.5

We performed three sets of simulations as listed below.

Simulation set A : We only change the mass of particles 2(M)

Simulation set B : We only change the interaction parameter between particle 2(ε_{22})

Simulation set C : We vary the mass of particles 2 to 16.0 and change the temperature (T)

2.3 Simulation for transport coefficient

2.3.1 Molecular dynamics method

There are molecular dynamics method and Monte Carlo method for simulations for liquids, solids, and dense gases. Among them, the molecular dynamics method is a simulation that determines the next motion of many particles from the initial position and the velocity according to the Newton's equation of motion. In our simulations, the velocity at each times is determined so that the total momentum becomes zero, and the temperature is set to be a temperature far from the phase transition temperature[16]. Periodic boundary conditions are used to minimize the effects of surfaces.

2.3.2 Velocity Verlet

For Molecular Dynamics (MD)simulations, Verlet method[17] is used for numerically solving Newton's equation of motion. This method uses Taylor expansion for the time evolution of the position and the velocity. In this study, we define mass m, time t, coordinate $r(t)$, velocity$v(t)$ and force $f(r,t)$. we rewrite the position, the velocity, and the force using the discrete-time variables, $r^n = r(t_n)$, $v^n = v(t_n)$, $f^n = f(r^n, t_n)$. The velocity Verlet scheme gives the time-marching equations as follows,

$$r^{n+1} = r^n + v^n dt + \frac{dt^2}{2m} f^n \tag{2.2}$$

$$v^{n+1} = v^n + \frac{dt}{2m}(f^n + f^{n+1}). \tag{2.3}$$

Using the above calculation scheme, the position and velocity are updated every discrete time step.

2.4 Deviation of transport coefficient

For the temperature gradient, there are various methods [18]. The frequently used method is arranging heat baths on both sides of the system. However, if the temperature gradient is directly applied in such a way non-linear effects such

as convention may occur, which makes theoretical analysis difficult. Evans[12][11] determined transport coefficients by using Green-Kubo formula in equilibrium state. Green-Kubo formula is the relation between the fluctuations of the system and transport coefficient. We employ this approach make the system simpler, we determined the transport coefficients in equilibrium state.

2.4.1 The relationship between energy and standard deviation

Standard deviation is written as

$$\sigma^2 = \langle E^2 \rangle - \langle E \rangle^2, \tag{2.4}$$

where σ^2 is the standard deviation, energy E. By using ($\beta = \frac{1}{k_B T}$), the standard deviation of energy satisfies

$$\frac{\partial U}{\partial \beta} = -\left(\langle E^2 \rangle - \langle E \rangle^2\right), \tag{2.5}$$

where U is the internal energy By using equations eq. (2.4) and eq. (2.5), we have

$$\sigma^2 = -\frac{\partial U}{\partial \beta} = k_B T^2 \left.\frac{\partial U}{\partial T}\right|_{V,N} = k_B T^2 C_V. \tag{2.6}$$

From this equation, specific heat can be written as1

$$C_V = \frac{1}{k_B T^2}\sigma^2. \tag{2.7}$$

2.4.2 Pressure Tensor

Pressure tensor is derived from the momentum density balance [19][20], which can be written as

$$\frac{\partial(\rho \boldsymbol{v})}{\partial t} = -\nabla \cdot [\boldsymbol{P} + \rho \boldsymbol{v}\boldsymbol{v}] + \rho \boldsymbol{F}^e. \tag{2.8}$$

The first Fourier gives

$$\frac{\partial}{\partial t}[\widetilde{\rho \boldsymbol{v}}(\boldsymbol{k},t)] = i\boldsymbol{k} \cdot \tilde{\boldsymbol{P}}(\boldsymbol{k},t) + i\boldsymbol{k} \cdot [\widetilde{\rho \boldsymbol{v}\boldsymbol{v}}(\boldsymbol{k},t)] + \widetilde{\rho \boldsymbol{F}^e}(\boldsymbol{k},t), \tag{2.9}$$

where the Fourier transform of function f(x) is defined as

$$Ff(x) = \tilde{f}(k) = \int_{-\infty}^{\infty} e^{ikx} f(x) dx. \tag{2.10}$$

Let us define the force in the system. The total force acting on atom i includes three different forces as follows

1. intermolecular forces :$\boldsymbol{F}_i^{\phi}$
2. constraint forces :$\boldsymbol{F}_i^{C}$
3. any synthetic forces :$\boldsymbol{F}_i^{e}$

The total force can be written as

$$\boldsymbol{F}_i = \boldsymbol{F}_i^{\phi} + \boldsymbol{F}_i^{C} + \boldsymbol{F}_i^{e}. \tag{2.11}$$

We take the Fourier transform of the microscopic expression for the momentum density, and evaluate the left-hand side of eq. (2.9)

$$\begin{aligned} \frac{\partial}{\partial t}[\widetilde{\rho \boldsymbol{v}}(\boldsymbol{k},t)] &= \frac{\partial}{\partial t}\sum_{i=1}^{N} m_i \boldsymbol{v}_i e^{i\boldsymbol{k}\cdot\boldsymbol{r}_i} \\ &= \sum_{i=1}^{N} m_i(\boldsymbol{v}_i + i\boldsymbol{k}\cdot\boldsymbol{v}_i\boldsymbol{v}_i)e^{i\boldsymbol{k}\cdot\boldsymbol{r}_i}, \end{aligned} \tag{2.12}$$

where we have take the Fourier transform for the first term in the right-hand side. Using the equation eq. (2.11), use the Taylor expansion as

$$\sum_{i=1}^{N} \boldsymbol{F}_i^{\phi} e^{i\boldsymbol{k}\cdot\boldsymbol{r}_i} = i\boldsymbol{k}\cdot\sum_{i=1}^{N} \boldsymbol{r}_i\boldsymbol{F}_i^{\phi} + \mathscr{O}(k^2), \tag{2.13}$$

$$\sum_{i=1}^{N} \boldsymbol{F}_i^{C} e^{i\boldsymbol{k}\cdot\boldsymbol{r}_i} = i\boldsymbol{k}\cdot\sum_{i=1}^{N} \boldsymbol{r}_i\boldsymbol{F}_i^{C} + \mathscr{O}(k^2). \tag{2.14}$$

Now we consider the convective term in the momentum balance equation. Let us introduce

$$\boldsymbol{c}_i = \boldsymbol{v}_i - \boldsymbol{v}(\boldsymbol{r}_i), \tag{2.15}$$

where $\boldsymbol{v}_i$ is the velocity of particle i relative to the laboratory frame and $\boldsymbol{v}_i(\boldsymbol{r}_i)$ is the streaming velocity at the position of atom i. By using above definition , we rewrite the second term of the right-hand side of eq. (2.9) as

$$\sum_{i=1}^{N} m_i\boldsymbol{v}_i\boldsymbol{v}_i e^{i\boldsymbol{k}\cdot\boldsymbol{r}_i} = i\boldsymbol{k}\cdot\sum_{i=1}^{N} m_i[\boldsymbol{c}_i\boldsymbol{c}_i + \boldsymbol{v}(\boldsymbol{r}_i)\boldsymbol{v}(\boldsymbol{r}_i)] + \mathscr{O}(k^2). \tag{2.16}$$

From eq. (2.9) we rewrite the pressure tensor as below

$$\begin{aligned} i\boldsymbol{k}\cdot\tilde{\boldsymbol{P}}(\boldsymbol{k},t) &= \frac{\partial}{\partial t}[\widetilde{\rho\boldsymbol{v}}(\boldsymbol{k},t)] - i\boldsymbol{k}\cdot[\widetilde{\rho\boldsymbol{v}\boldsymbol{v}}(\boldsymbol{k},t)] - \widetilde{\rho\boldsymbol{F}^e}(\boldsymbol{k},t) \\ &= i\boldsymbol{k}\cdot\left(\sum_{i=1}^{N} m_i\boldsymbol{c}_i\boldsymbol{c}_i + \sum_{i=1}^{N}\boldsymbol{r}\boldsymbol{F}_i^{\phi} + \sum_{i=1}^{N}\boldsymbol{r}\boldsymbol{F}_i^{C}\right) + \mathscr{O}(k^2). \end{aligned} \tag{2.17}$$

Now we consider a divergence less quantity for the zero-wavevector($\boldsymbol{k}=0$) pressure tensor

$$\tilde{\boldsymbol{P}}(\boldsymbol{k}=0,t) = V\boldsymbol{P}(t) = \sum_{i=1}^{N} m_i\boldsymbol{c}_i\boldsymbol{c}_i + \sum_{i=1}^{N}\boldsymbol{r}\boldsymbol{F}_i^{\phi} + \sum_{i=1}^{N}\boldsymbol{r}\boldsymbol{F}_i^{C}. \tag{2.18}$$

In this study, because we do not consider constraint forces, the final expression of the pressure tensor is written as

$$V\boldsymbol{P}(t) = \sum_{i=1}^{N} m_i\boldsymbol{c}_i\boldsymbol{c}_i - \frac{1}{2}\sum_{i=1}^{N}\sum_{i\neq j}^{N}\boldsymbol{r}_{ij}\boldsymbol{F}_{ij}^{\phi}. \tag{2.19}$$

2.4.3 Energy balance equation

The total energy of the mass element, $e(\boldsymbol{r},t)\delta m$, consists of four elements as listed below

1. kinetic energy of the centre of mass,
2. the macroscopic potential energy of the mass element due to its interactions with external conservative fields $\delta m\psi$
3. the microscopic kinetic energy due to the atomic motion relative to the centre of mass
4. the microscopic potential energy according the interatomic forces

$$e\delta m = \frac{1}{2}\delta m v^2 + \psi\delta m + u\delta m. \tag{2.20}$$

where the centre of velocity v, mass m, the last two are combined into the internal energy $u\delta m$.
Taking the time derivative of eq. (2.20), dividing by the volume of δm, and taking the infinitesimal limit, We have the rate of change of the specific energy as

$$\rho\frac{de}{dt} = \frac{1}{2}\rho\frac{dv^2}{dt} + \rho\frac{d\psi}{dt} + \rho\frac{du}{dt}. \tag{2.21}$$

The first term on the right-hand side of eq. (2.21) is

$$\frac{1}{2}\rho\frac{dv^2}{dt} = -\boldsymbol{v}\cdot(\nabla\cdot\boldsymbol{P}) + \rho\boldsymbol{v}\cdot\boldsymbol{F}^e. \tag{2.22}$$

The second term on the right-hand side of eq. (2.21) is

$$\rho\frac{d\psi}{dt} = \rho\boldsymbol{v}\cdot\nabla\psi = -\rho\boldsymbol{v}\cdot\boldsymbol{F}^e. \tag{2.23}$$

On the left-hand side of eq. (2.21), the total energy of the mass element can only change the work done by the stress and nonconservative external forces. The rate of change of the total energy is expressed as

$$\rho\frac{de}{dt} = \rho\frac{dw^t}{dt} + \rho\frac{dq}{dt}, \tag{2.24}$$

where w^t is the specific mechanical work done by the stresses and q is the specific heat absorption. The first term and second terms in the right-hand side of eq. (2.24) can be expressed in terms of the thermal diffusion flux ($\boldsymbol{J}_q$) and the pressure ($\boldsymbol{P}$) as

$$\rho\frac{dw^t}{dt} = -\nabla\cdot(\boldsymbol{P}\cdot\boldsymbol{v}) \tag{2.25}$$

$$\rho\frac{dq}{dt} = -\nabla\cdot\boldsymbol{J}_q. \tag{2.26}$$

By using($\nabla\cdot(\boldsymbol{P}\cdot\boldsymbol{v}) = \nabla\cdot\boldsymbol{P}\cdot\boldsymbol{v} + \boldsymbol{P}^T : \nabla\boldsymbol{v}$), the total energy satisfies

$$\begin{aligned}\rho\frac{de}{dt} &= \rho\frac{dw^t}{dt} + \rho\frac{dq}{dt} - \frac{1}{2}\rho\frac{dv^2}{dt} - \rho\frac{d\psi}{dt}\\ &= -\nabla\cdot(\boldsymbol{P}\cdot\boldsymbol{v}) - \nabla\cdot\boldsymbol{J}_q + \boldsymbol{v}\cdot(\nabla\cdot\boldsymbol{P})\\ &= -\nabla\cdot\boldsymbol{J}_q - \boldsymbol{P}^T : \nabla\boldsymbol{v}.\end{aligned} \tag{2.27}$$

2.4.4 Heat flux vector

We convert the total derivative to the partial derivative for the right-hand of eq. (2.27) as

$$\begin{aligned}\rho\frac{de}{dt} &= -\nabla\cdot\boldsymbol{J}_q - \boldsymbol{P}^T : \nabla\boldsymbol{v},\\ \rho\frac{\partial e}{\partial t} &= -\nabla\cdot[\boldsymbol{J}_q + \rho e\boldsymbol{v} + \boldsymbol{P}\cdot\boldsymbol{v}],\end{aligned} \tag{2.28}$$

the Fourier transform of eq. (2.28) is written as

$$\frac{\partial}{\partial t}[\widetilde{\rho e}(\boldsymbol{k},t)] = i\boldsymbol{k}\cdot\tilde{\boldsymbol{J}}_q(\boldsymbol{k},t) + i\boldsymbol{k}\cdot[\widetilde{\rho e\boldsymbol{v}}(\boldsymbol{k},t)] + i\boldsymbol{k}\cdot[\widetilde{\boldsymbol{P}\cdot\boldsymbol{v}}(\boldsymbol{k},t)]. \tag{2.29}$$

The time derivative of the transformed energy density can be written as

$$\begin{aligned}\frac{\partial}{\partial t}[\widetilde{\rho e}(\boldsymbol{k},t)] &= \frac{\partial}{\partial t}\sum_i e_i e^{i\boldsymbol{k}\cdot\boldsymbol{r}_i}\\ &= \sum_i \dot{e}_i e^{i\boldsymbol{k}\cdot\boldsymbol{r}} + i\boldsymbol{k}\cdot\sum_i e_i\boldsymbol{v}_i e^{i\boldsymbol{k}\cdot\boldsymbol{r}_i},\end{aligned} \tag{2.30}$$

where e_i is written as ($e_i = \frac{1}{2}m_i v_i^2 + \frac{1}{2}\sum_j \phi_{ij}$). The first term of the right-hand side of eq. (2.30) is

$$\begin{aligned}\sum_i \dot{e}_i e^{i\boldsymbol{k}\cdot\boldsymbol{r}_i} &= \sum_i \boldsymbol{v}_i\cdot\boldsymbol{F}_i e^{i\boldsymbol{k}\cdot\boldsymbol{r}_i} - \frac{1}{2}\sum_i\sum_{j\neq i}(\boldsymbol{F}_{ij}^\phi\cdot\boldsymbol{v}_i + \boldsymbol{F}_{ji}^\phi\cdot\boldsymbol{v}_j)e^{i\boldsymbol{k}\cdot\boldsymbol{r}_i}\\ &= \frac{1}{2}\sum_i\sum_j(\boldsymbol{F}_{ij}^\phi\cdot\boldsymbol{v}_i - \boldsymbol{F}_{ji}^\phi\cdot\boldsymbol{v}_j)e^{i\boldsymbol{k}\cdot\boldsymbol{r}_i}\\ &= \frac{1}{2}\sum_i\sum_{j\neq i}\boldsymbol{F}_{ij}^\phi\cdot\boldsymbol{v}_i(e^{i\boldsymbol{k}\cdot\boldsymbol{r}_i} - e^{i\boldsymbol{k}\cdot\boldsymbol{r}_j}).\end{aligned} \tag{2.31}$$

In this study, because we do not consider nonconservative external forces and the lowest order in the wavevector, eq. (2.31) becomes

$$\sum_i \dot{e}_i e^{i\boldsymbol{k}\cdot\boldsymbol{r}_i} = i\boldsymbol{k}\cdot\left(\sum_i \boldsymbol{r}_i\cdot\boldsymbol{F}_i^C\cdot\boldsymbol{v}_i - \frac{1}{2}\sum_i\sum_{i\neq j}\boldsymbol{r}_{ij}\cdot\boldsymbol{F}_{ij}^{\phi}\cdot\boldsymbol{v}_i\right) + \mathscr{O}(k^2). \tag{2.32}$$

The second term of the right-hand side of eq. (2.29) is written as

$$i\boldsymbol{k}\cdot[\rho\tilde{e}\boldsymbol{v}(\boldsymbol{k},t)] = i\boldsymbol{k}\cdot\sum_i e_i\boldsymbol{v}(\boldsymbol{r}_i,t)e^{i\boldsymbol{k}\cdot\boldsymbol{r}_i}. \tag{2.33}$$

The third term of the right-hand side of eq. (2.29) is the work done by the pressure tensor. From eq. (2.19), we obtain

$$i\boldsymbol{k}\cdot\widetilde{\boldsymbol{P}\cdot\boldsymbol{v}}(\boldsymbol{k},t) = i\boldsymbol{k}\cdot F\left\{\left[\sum_i m_i\boldsymbol{c}_i\boldsymbol{c}_i\delta(\boldsymbol{r}-\boldsymbol{r}_i) - \frac{1}{2}\sum_i\sum_{j\neq i}\boldsymbol{r}_{ij}\boldsymbol{F}_{ij}^{\phi}\right]\cdot\boldsymbol{v}(\boldsymbol{r}_i)\right\}. \tag{2.34}$$

We separate the kinetic part and the potential part, The work done by the pressure tensor is written as

$$i\boldsymbol{k}\cdot\widetilde{\boldsymbol{P}^K\cdot\boldsymbol{v}}(\boldsymbol{k},t) = i\boldsymbol{k}\cdot\sum_i m_i\boldsymbol{c}_i\boldsymbol{c}_i\cdot\boldsymbol{v}(\boldsymbol{r}_i,t) + \mathscr{O}(k^2), \tag{2.35}$$

$$i\boldsymbol{k}\cdot\widetilde{\boldsymbol{P}^{\phi}\cdot\boldsymbol{v}}(\boldsymbol{k},t) = -\frac{1}{2}i\boldsymbol{k}\cdot\sum_i\sum_{j\neq i}\boldsymbol{r}_{ij}\boldsymbol{F}_{ij}^{\phi}\cdot\boldsymbol{v}(\boldsymbol{r}_i) + \mathscr{O}(k^2). \tag{2.36}$$

Substituting the result of the above formula into the energy balance equation, we obtain the heat flux of the kinetic part as

$$V\tilde{\boldsymbol{J}}_q^K(t) = \sum_i e_i\boldsymbol{v}_i - \sum_i e_i\boldsymbol{v}(\boldsymbol{r}_i,t) - \sum_i m_i\boldsymbol{c}_i\boldsymbol{c}_i\cdot\boldsymbol{v}(\boldsymbol{r}_i,t) = \sum_i u_i\boldsymbol{c}_i, \tag{2.37}$$

and the configural part as

$$V\tilde{\boldsymbol{J}}_q^{\phi}(t) = -\frac{1}{2}\sum_i\sum_{i\neq j}\boldsymbol{r}_{ij}\boldsymbol{F}_{ij}^{\phi}\cdot\boldsymbol{c}_i. \tag{2.38}$$

In homogeneous systems, the heat flux can be expressed when we take the limit of the wavevector to 0. Then we have

$$V\boldsymbol{J}_q(t) = \sum_i u_i\boldsymbol{c}_i - \frac{1}{2}\sum_i\sum_{j\neq i}\boldsymbol{r}_{ij}F_{ij}^{\phi}\cdot\boldsymbol{c}_i. \tag{2.39}$$

2.4.5 Mass flux vector

We define the mass flux vector of particles 1 as

$$V\boldsymbol{J}_1(t) = \sum_i^{N_1} m_i\boldsymbol{v}_i. \tag{2.40}$$

Since the total momentum is 0, the norm of the mass flux of particles 2 is the same with that for particles 1 whereas the direction is opposite.

2.4.6 Green-Kubo formula

We derive the Grren-Kubo formula for the thermal conductivity[21]. We define the thermal flux $\boldsymbol{J}_Q$ and the thermal diffusivity by the following equations

$$\rho\frac{dU}{dt} = -\nabla\cdot\boldsymbol{J}_Q, \tag{2.41}$$

$$\boldsymbol{J}_Q = -\lambda\nabla^2 T. \tag{2.42}$$

From these equations, we have

$$\rho\frac{dU}{dt} = \lambda\nabla^2 T. \tag{2.43}$$

Time derivative of eq. (2.43) is written as

$$(\rho + \nabla\rho)\frac{(\langle U\rangle + \Delta U)}{dt} = \rho\frac{d\Delta U}{dt}. \tag{2.44}$$

Because temperature does not affect the total energy, we rewire eq. (2.43) as

$$\rho\frac{d\Delta U}{dt} = \lambda\nabla^2\Delta T. \tag{2.45}$$

The relation between the change of energy and the specific heat is written as

$$\frac{1}{V}\frac{\partial E}{\partial T}\bigg|_V = \frac{\partial \rho U}{\partial T}\bigg|_V = \rho c_v. \tag{2.46}$$

We rewire eq. (2.45) by using specific heat c_V as

$$\rho\Delta\dot{U} = \frac{\lambda}{\rho c_V}\nabla^2\rho\Delta U. \tag{2.47}$$

where we define $D_T = \frac{\lambda}{\rho c_V}$ and use Fourier transform to rewrite eq. (2.46) as

$$\rho\Delta\dot{U}(\boldsymbol{k},t) = -k^2 D_T\rho\Delta U(\boldsymbol{k},t). \tag{2.48}$$

The autocorrelation function $C(k,t)$ of the internal energy depending on the wavevector is written as

$$C(k,t) \equiv \langle\rho\Delta U(\boldsymbol{k},t)\rho\Delta U(-\boldsymbol{k},0)\rangle. \tag{2.49}$$

Hereafter, we regard to the wavevector as a scalar because the system is homogeneous. We use Laplace transform to eq. (2.48) to obtain the following form

$$\tilde{C}(k,\omega) = \frac{C(k,0)}{i\omega + k^2\tilde{D}_T(k,\omega)}. \tag{2.50}$$

Here,we define ϕ as

$$\phi(k,t) = \dot{C} = k^2\langle J_{Qx}(k,t)J_{Qx}(-k,0)\rangle. \tag{2.51}$$

Wavenumber dependence of the thermal diffusivity is written as

$$k^2\tilde{D}_T(k,\omega) = \frac{C(k,0) - i\omega\tilde{C}(k,\omega)}{\tilde{C}(k,\omega)} = \frac{\tilde{\phi}(k,\omega)}{C(k,0) - \frac{\tilde{\phi}(k,\omega)}{i\omega}}. \tag{2.52}$$

Finally, we take the limit of the wavenumber to 0 to rewrite eq. (2.7). By using the relation of $\left(\rho c_V = \frac{1}{k_B T^2}C(0,0)\right)$, we have the Grren-Kubo formula for thermal conductivity as

$$L_{qq} = \frac{V}{k_B}\int_0^\infty dx\langle J_{Qx}(0,t)J_{Qx}(0,0)\rangle. \tag{2.53}$$

Similarly, the autocorrelation function for the mass flux is given as

$$L_{11} = \frac{V}{k_B}\int_0^\infty dx\langle J_{1x}(0,t)J_{1x}(0,0)\rangle. \tag{2.54}$$

The crosscorrelation function for the fluxes of mass and heat is written as

$$L_{1q} = \frac{V}{k_B}\int_0^\infty dx\langle J_{1x}(0,t)J_{qx}(0,0)\rangle. \tag{2.55}$$

In this study, we define the autocorrelation function is for the fluxes of mass and heat as

$$C_{11}(t) = \langle J_{1x}(t)J_{1x}(0)\rangle. \tag{2.56}$$

$$C_{qq}(t) = \langle J_{qx}(t)J_{qx}(0)\rangle. \tag{2.57}$$

The cross-correlation function can be written as

$$C_{1q}(t) = \langle J_{1x}(t)J_{qx}(0)\rangle. \tag{2.58}$$

2.4.7 The relation between Soret coefficient and Onsager coefficient

The fluxes at a given point of space and at a given time are written as

$$\boldsymbol{J}_i(\boldsymbol{r},t) = \boldsymbol{J}_i\left[\mathscr{F}_1(\boldsymbol{r},t), \mathscr{F}_2(\boldsymbol{r},t), ...\right]. \tag{2.59}$$

This formula express the fact that each flux depend not only on its conjugate affinity but also on the other affinities. Near equilibrium, this formula is rewritten as

$$\boldsymbol{J}_i(\boldsymbol{r},t) = \sum_k L_{ik}\mathscr{F}_k(\boldsymbol{r},t), \tag{2.60}$$

where $L_{ik} = \frac{\partial \boldsymbol{J}_i}{\partial \mathscr{F}_k}$ and $\mathscr{F}$ is the intensive generalized forces, and L_{ik} is the matrix of the kinetic coefficients characterizing the linear response. The linear phenomenological equations can be written as

$$\boldsymbol{J}_q = -L_{qq}\boldsymbol{X}_q - L_{q1}\boldsymbol{X}_1, \tag{2.61}$$

$$\boldsymbol{J}_1 = -L_{11}\boldsymbol{X}_1 - L_{1q}\boldsymbol{X}_q, \tag{2.62}$$

where $\boldsymbol{J}_q$ is the heat flux, $\boldsymbol{J}_1$ is the mass flux, L_{ij} is the Onsager coefficients and $\boldsymbol{X}$ is the thermodynamic forces. The practical transport coefficients are defined by

$$\boldsymbol{J}_q = -\lambda\Delta T - \rho_1\frac{\partial\mu_1}{\partial c_1}TD''\Delta c_1, \tag{2.63}$$

$$\boldsymbol{J}_1 = -\rho D\Delta c_1 - \rho c_1 c_2 D'\Delta T, \tag{2.64}$$

where D is the mutual diffusion coefficient, D' is the thermal diffusion coefficient, D'' is the Dufour coefficient and λ is the thermal conductivity. By using two above phenomenological equations, we summarize the relation between Soret coefficients and Onsager coefficients.

$$D = \frac{L_{11}}{\rho c_2 T}\left(\frac{\partial\mu_1}{\partial c_1}\right) \tag{2.65}$$

$$D' = \frac{L_{1q}}{\rho c_1 c_2 T^2} \tag{2.66}$$

$$D'' = \frac{L_{q1}}{\rho c_1 c_2 T^2} \tag{2.67}$$

$$\lambda = \frac{L_{qq}}{T^2} \tag{2.68}$$

$$S_T = \frac{D}{D'}, \tag{2.69}$$

where S_T is the Soret coefficient.

2.5 Data analysis

2.5.1 Radial distribution function

We define the radial distribution function as

$$g_{ij}(r) = \frac{\text{the number of particles which locate from } r \text{ to } r+\Delta r}{\rho\frac{4\pi}{3}\left[(r+\Delta r)^3 - r^3\right]}, \tag{2.70}$$

where $g_{ij}(r)$ is the radial distribution function of particle i and particle j, ρ is the density.

2.5.2 Mean square displacement

We define the mean square displacement(MSD) as

$$\mathrm{MSD}_{ij}(t) = \left\langle(\boldsymbol{r}_i(t) - \boldsymbol{r}_j(0)\rangle\right)^2, \tag{2.71}$$

where $(\boldsymbol{r}_i(t) - \boldsymbol{r}_j(0))$ is the distance from the particles j at time 0 to the particles i at time t.

Chapter 3

Result and Discussion

3.1 Mass dependence

We calculate the C_{11}, the C_{qq} and the C_{1q} with varying M. We performed the simulation set A.

3.1.1 Heat autocorrelation function

By using eq. (2.39), we calculate the heat flux.
The autocorrelation function of the heat flux of WCA potential and LJ potential is shown below. When $M = 1$, the

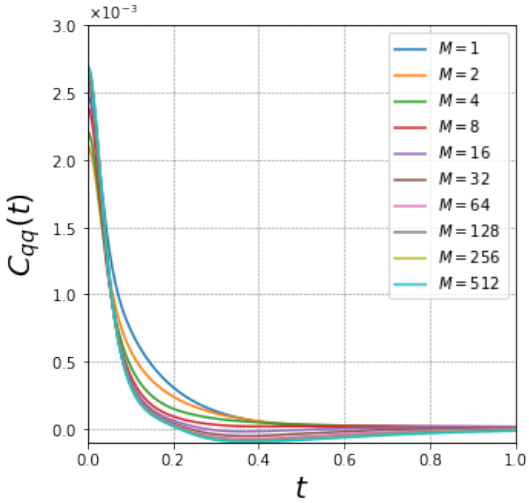

Figure 3.1: C_{qq} for WCA potential with various M values

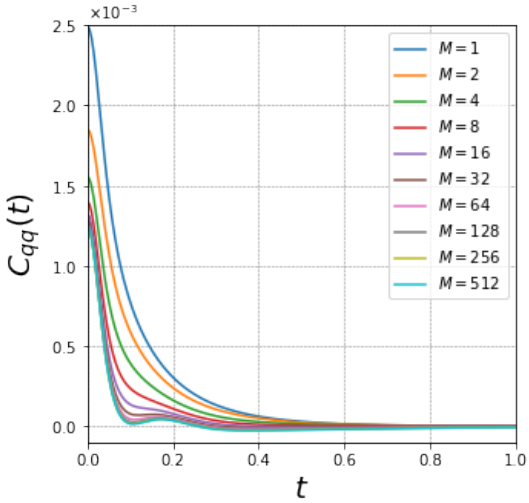

Figure 3.2: C_{qq} function for LJ potential with various M values

heat autocorrelation function monotonically decays and the relaxation time is ca 0.2. For the case of $M = 512$, the LJ potential showed the fast relaxation that almost completes around $t = 0.1$ followed by a small oscillatory damp. The WCA potential showed a two-step relaxation reflecting the relaxation of heavy and light particles. It was also found that the correlation function of the LJ potential does not have a negative value, whereas that of the WCA potential has a negative value when the mass contrast is large.

From the results shown in C_{qq} and using the Green-Kubo formula defined eq. (2.53), we calculate the transport coefficients of the heat flux.

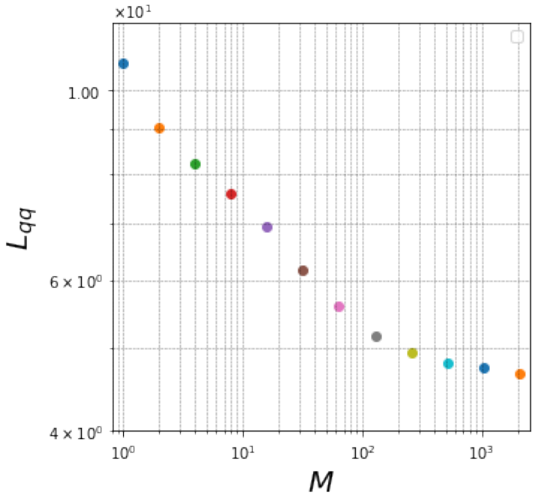

Figure 3.3: L_{qq} for WCA potential with various M values

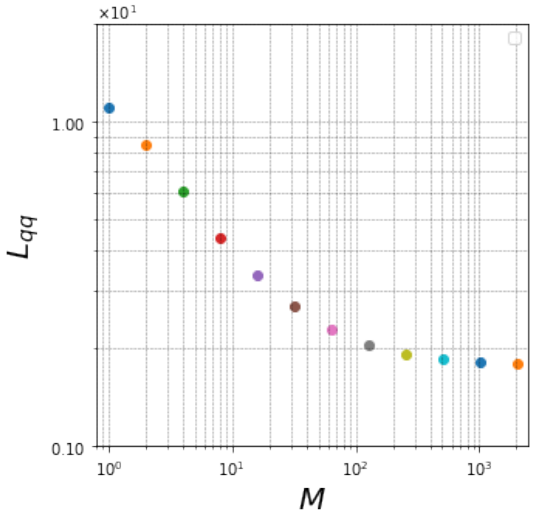

Figure 3.4: L_{qq} for LJ potential with various M values

It was found that the heat transport coefficient decreases as the contrast of mass increases for each potential. In other words, the heavy particles suppress the heat flow. It was also found that the heat transport coefficient converged to a certain value as the mass ratio increases.

3.1.2 Mass autocorrelatin function

By using equation eq. (2.40), we calculate the mass flux $\boldsymbol{J}_1$ and the autocorrelation function of the mass flux C_{11} of WCA potential and LJ potential is shown below.

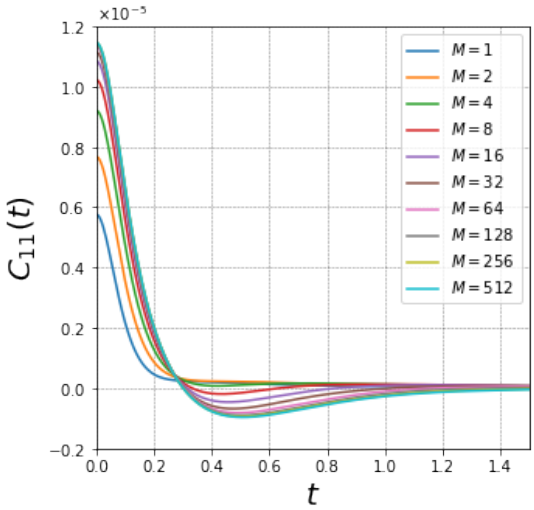

Figure 3.5: C_{11} for WCA potential with various M values

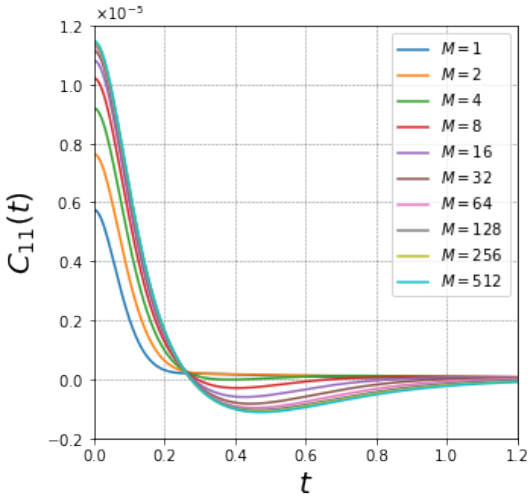

Figure 3.6: C_{11} for LJ potential with various M values

For $M = 1$, the mass autocorrelation function at $t = 0$ is $\frac{3}{2}k_BT$. The mass autocorrelation function decays monotonically and the relaxation time is ca 0.2. As the mass contrast increases, the mass autocorrelation function at $t = 0$ is increased by constraint of center of mass velocity is 0[see Appendix]. Concerning the effect of the potentials, it seems that the undershoot to negative value is intense for LJ rather than WCA potentials.

From the results shown in C_{11} and by using the Green-Kubo formula eq. (2.54), we calculate the transport coefficients of mass flux L_{11}.

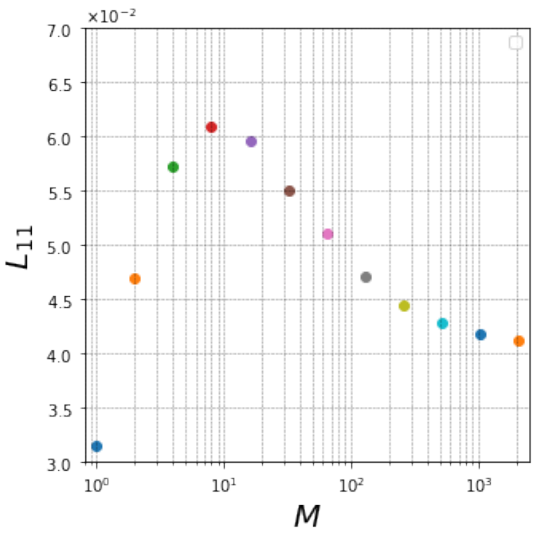

Figure 3.7: L_{11} for WCA potential with various M values

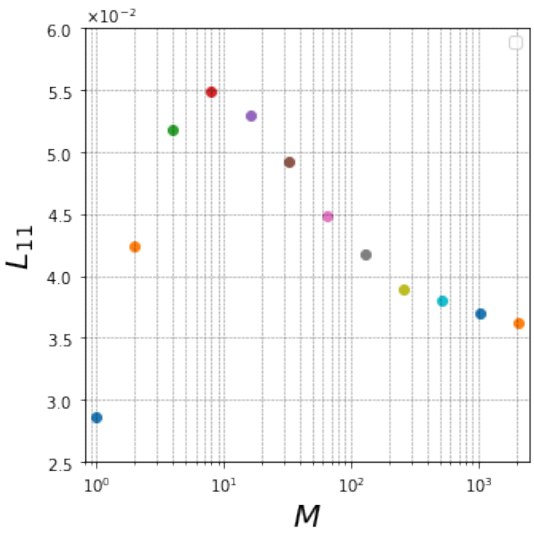

Figure 3.8: L_{11} for LJ potential with various M values

The transport coefficient of the mass flux increases as the contrast of mass increases in small M region, irrespective of the potential. Around M 10, L_{11} has a peak and decreases with increasing M. Then L_{11} converges to a certain value.

3.1.3 mass and heat crosscorrelation function

By using equation eq. (2.40) and eq. (2.39),we calculate mass and heat crosscorrelation function of the fluxes C_{1q}.

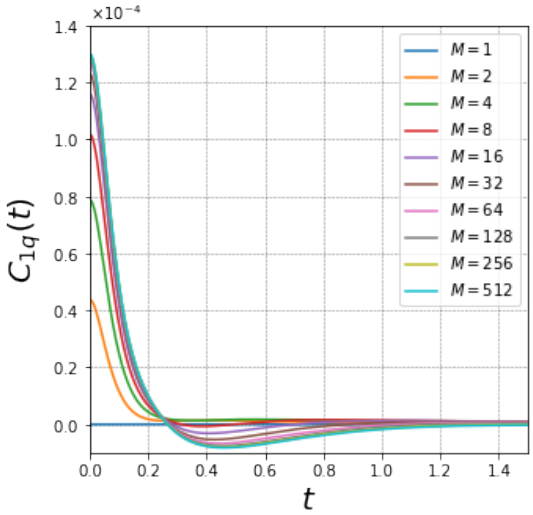

Figure 3.9: C_{1q} for WCA potential with various M values

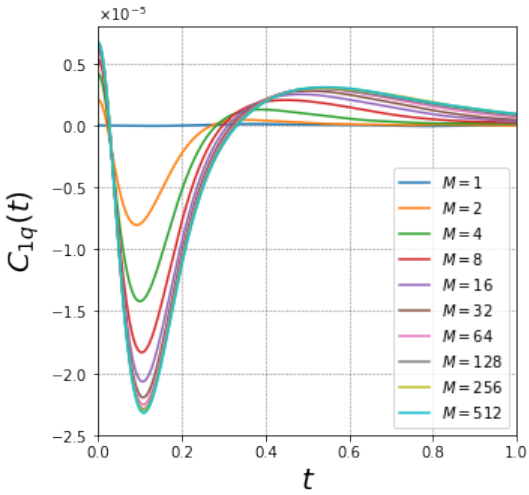

Figure 3.10: C_{1q} for LJ potential with various M values

When $M = 1$, the mass and heat crosscorrelation function is 0 because of the symmetry. When we increase M, the C_{1q} strongly depends on M. For the WCA potential, the C_{1q} shows the negative peaks at $t = 0.4$, whereas for the LJ potential C_{1q} shows the negative peaks at $t = 0.1$ and migrate to zero with damped oscillation. From the results in C_{1q} and by using the Green-Kubo formula shown in eq. (2.55), we calculate mass and heat cross transport coefficients L_{1q}.

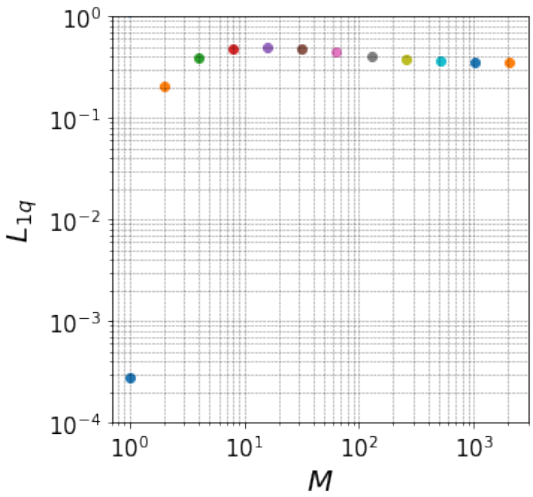

Figure 3.11: L_{1q} for WCA potential with various M values

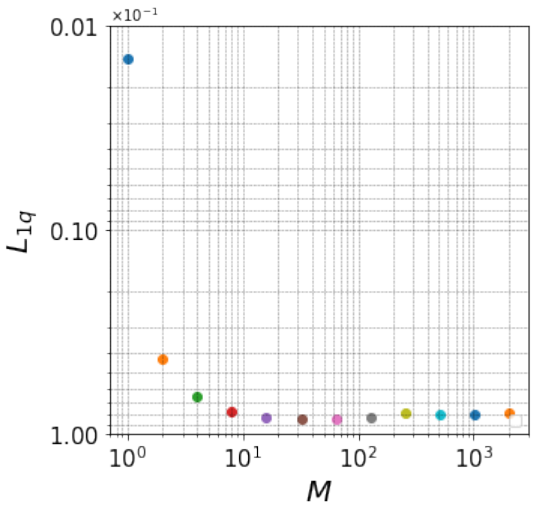

Figure 3.12: L_{1q} for LJ potential with various M values

L_{1q} for the LJ potential decreases with increasing the mass of particle 2, which means that particle with lighter mass move to the higher temperature side. This is the same result as the previous the report. On the other hand, L_{1q} for the WCA potential increases with increasing the mass, and it was found that the particles with light mass move to the lower temperature side.

3.1.4 Radial distribution function

To check if the structure has changed due to the difference in potential, we calculate radial distribution function(rdf) eq. (2.70) in each systems.

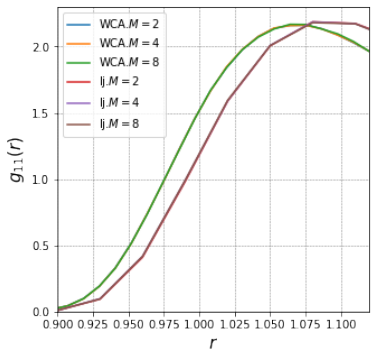

Figure 3.13: rdf of between particles 1 1

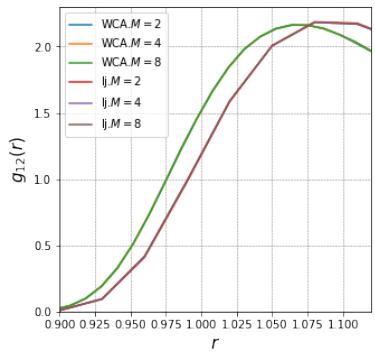

Figure 3.14: rdf of between particles 1 2

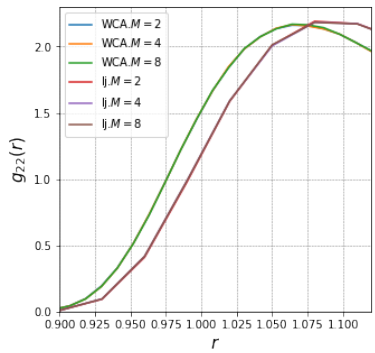

Figure 3.15: rdf of between particles 2 2

In each potentials, the radial distribution function is not depends on mass ,we can confirm that radial distribution function is same if potential is same. The first peak of WCA potential is closer than the first peak of LJ potential. Thus.the average of distance of WCA particles is closer than LJ particles.

3.1.5 Mean square displacement

When the mass difference is sufficient($M = 2048$), we calculate mean square displacement eq. (2.71) to check if the diffusion has changed due to the difference in potential.

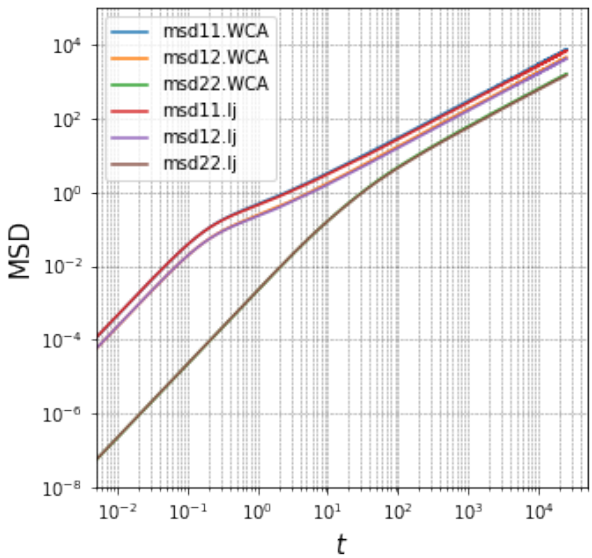

Figure 3.16: Mean square displacement of the particles

We can see the relaxation time is different from mass difference. When we consider the mean square displacement of particles 1, we can see case effect of the heavy particles(particles 2) Of course, Heavy particles have slow relaxation time, but there is no difference in each potential.

3.1.6 Discussion

When the simulation was performed using the mass of particle 2 as a parameter while keeping the mass of particle 1 at 1.0, it was found that the mass dependence of the cross-transportation coefficient differs between the WCA potential and the LJ potential. This result revealed that the presence or absence of attractive force reverses the mass dependence of the transport coefficient. However, by Vogelsang et al[13], the Soret coefficients in a repulsive system whose potential is proportional to (r^{-12}) differs from our result. It turns out that this difference is due to the definition of heat.

Heat flux used by Vogelsang is

$$\boldsymbol{J}_Q(t) = \sum_i u_i \boldsymbol{c}_i - \frac{1}{2}\sum_i \sum_{j\neq i} \boldsymbol{r}_{ij} F_{ij}^{\phi} \cdot \boldsymbol{c}_i - \sum_i h \boldsymbol{v}_i, \tag{3.1}$$

where h is partial enthalpy. The heat flux we used is the heat flux without enthalpy that defined by Irving-Kirkwood[20] Therefore, the result was different from ours depending on whether the effect of enthalpy was included or not. Even though the definition of heat flux is the sum of the flows of micro things, it remains a question whether it is good to include the flow of enthalpy, which is a macro quantity, into the same equation. Evans et al[12] reported that the enthalpy effect is negligible for linear response, our result is correct among linear response. It was considered that the transport coefficient in the repulsive system may have different results in the linear range and the non-linear range.

In addition, since the mass dependence of the transport coefficient changed due to the intermolecular potential difference, even if we consider the radial distribution function and the mean square displacement, there were no clear difference between the potentials. we thought that analysis by another approach would be necessary. The cross-correlation coefficient is derived from the cross-correlation function of heat flux and mass flux. Therefore, by decomposing the heat flux into a kinetic part and a potential part, we investigate the effect of the presence or absence of attractive force by investigating which part has a dominant effect on the value of the overall correlation function. We decompose into kinetic part and potential part.

$$V\boldsymbol{J}_q(t) = \sum_{\nu=1}^{1}\sum_{i=1}^{N_\nu} \frac{\boldsymbol{P}_{\nu i}}{m_\nu} \cdot \left[u_{\nu i}\mathbf{1} - \frac{1}{2}\sum_{\mu=1}^{r}\sum_{j=1}^{N_\mu} \boldsymbol{F}_{\nu i\mu j}\boldsymbol{r}_{\nu i\mu j} \right] \tag{3.2}$$

$$= \sum_{\nu=1}^{1}\sum_{i=1}^{N_\nu} \frac{\boldsymbol{P}_{\nu i}}{m_\nu} \cdot \left[\frac{1}{2} m_\nu \boldsymbol{v}_{\nu i\mu j}^2 + \Phi - \frac{1}{2}\sum_{\mu=1}^{r}\sum_{j=1}^{N_\mu} \boldsymbol{F}_{\nu i\mu j}\boldsymbol{r}_{\nu i\mu j} \right] \tag{3.3}$$

where we define the kinetic part of heat flux

$$V\boldsymbol{J}_q^K(t) = \sum_{\nu=1}^{1}\sum_{i=1}^{N_\nu} \frac{\boldsymbol{P}_{\nu i}}{m_\nu} \cdot \left[\frac{1}{2} m_\nu \boldsymbol{v}_{\nu i\mu j}^2 \right], \tag{3.4}$$

where we define the potential part of heat flux

$$V\boldsymbol{J}_q^P(t) = \sum_{\nu=1}^{1}\sum_{i=1}^{N_\nu} \frac{\boldsymbol{P}_{\nu i}}{m_\nu} \cdot \left[\Phi - \frac{1}{2}\sum_{\mu=1}^{r}\sum_{j=1}^{N_\mu} \boldsymbol{F}_{\nu i\mu j}\boldsymbol{r}_{\nu i\mu j} \right]. \tag{3.5}$$

By using two heat fluxes and eq. (2.39), we calculate heat autocorrelation function of each part in WCA potential.

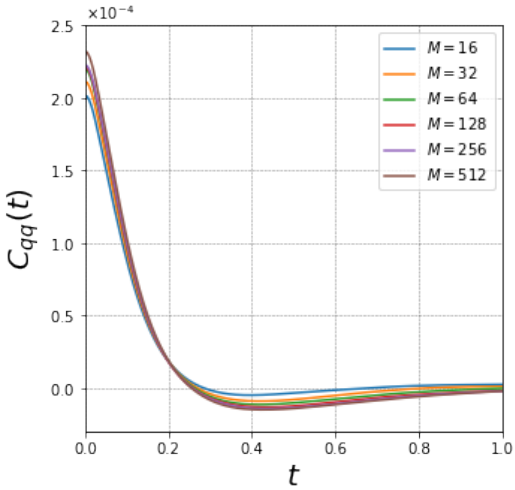

Figure 3.17: C_{qq} for LJ potential of kinetic part with various M values

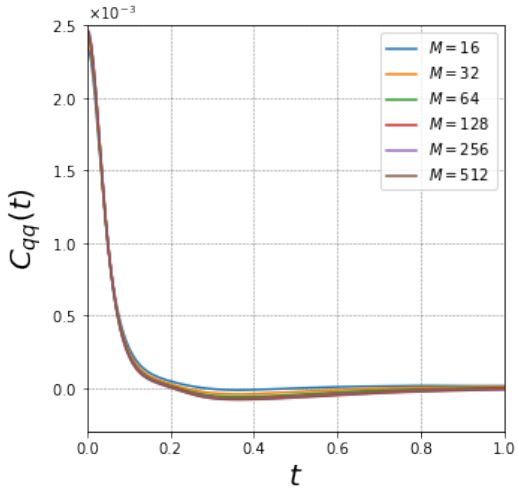

Figure 3.18: C_{qq} for LJ potential of potential part with various M values

We thought that the two-step relaxation depend on the potential part. In addition, this two-step relaxation can be divided into three categories: the collision time when the particles motion is not significantly affected by the potential and the time when the particles motion is affected by the potential and the time after when the particles motion is affected by the potential. Therefore, it was considered that two-step relaxation was seen.

We consider the difference of heat and mass transport coefficients between two potentials by using the eq. (2.55). We calculate the heat and mass crosscorrelation function of kinetic part for each potential.

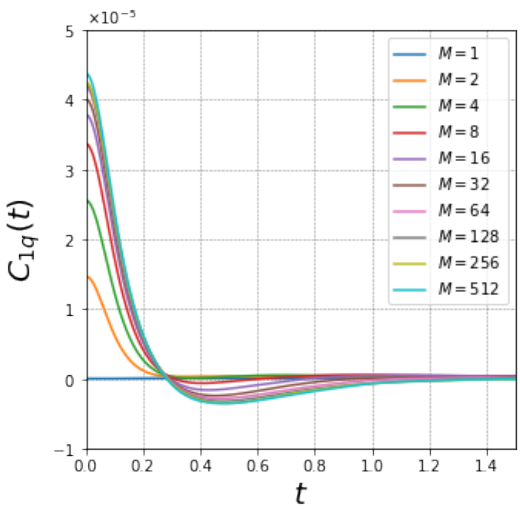

Figure 3.19: C_{1q} for WCA potential of kinetic part with various M values

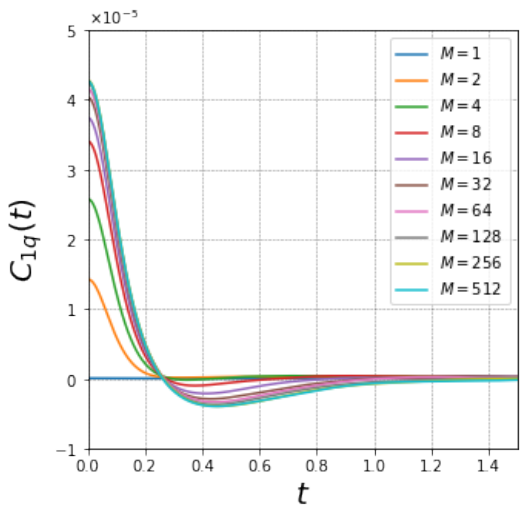

Figure 3.20: C_{1q} for LJ potential of kinetic part with various M values

When $M = 1$, the heat and mass crosscorrelation function is 0 due to the symmetry. When we change the M, we found that the heat and mass crosscorrelation function have same behavior in each potential. The transport of kinetic part does not depend on the attractive forces.

We calculate the heat and mass crosscorrelation function of kinetic part for each potential.

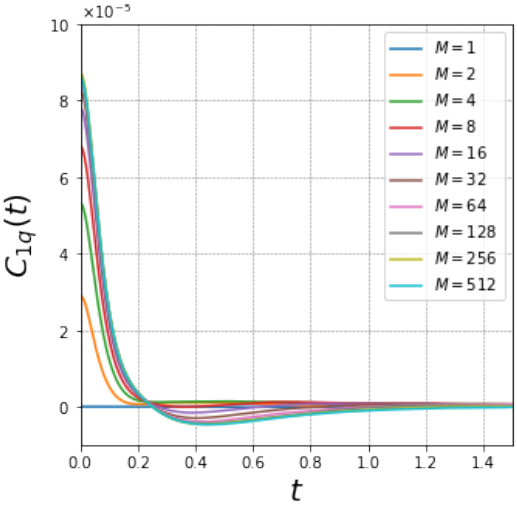

Figure 3.21: C_{1q} for WCA potential of potential part with various M values

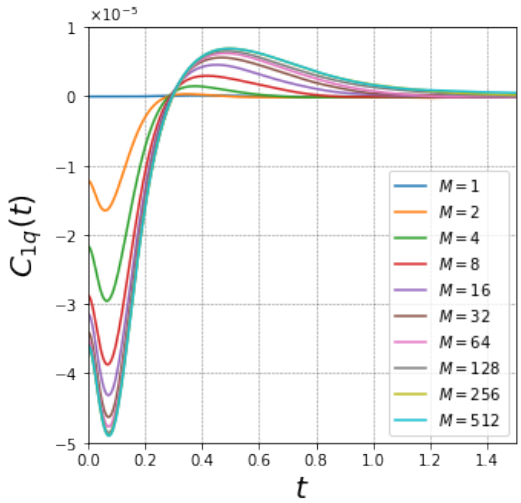

Figure 3.22: C_{1q} for LJ potential of potential part with various M values

When $M = 1$, the heat and mass cross transport coefficient is 0 due to the symmetry. When we change the M, the cross correlation function have positive sign at $t = 0$ in WCA potential whereas they have negative sign at $t = 0$. In WCA potential, the behavior of cross correlation function is same with momentum auto correlation function. In LJ potential, the crosscorrelation function have a small oscillatory damp. The difference of heat and mass cross correlation function of potential affect the heat and mass cross transport coefficients.

3.1.7 Conclusion

In this section, we investigate mass dependence of transport coefficient in each potentials. We summary the result in this section.

Purpose :
investigate the mass dependence of transport coefficient in each potentials

Result of WCA potential :
that particles with lighter mass move to the lower temperature side and that particles with heavier mass move to the higher temperature side

Result of LJ potential :
that particles with lighter mass move to the higher temperature side and that particles with heavier mass move to the lower temperature side

Consideration of rdf :
the first peak of WCA potential is closer than the first peak of LJ potential but maximal value is almost same in each potential

Consideration of MSD :
heavier particles have slow relaxation time and there no difference in each potential

Discussion :
The difference of heat and mass cross correlation function of potential affect the heat and mass cross transport coefficients.

3.2 Potential parameter dependence

We calculate the C_{11}, the C_{qq} and the C_{1q} with varying M. We performed the simulation set B.

3.2.1 Heat autocorrelation function

By using the eq. (2.39), we calculate heat flux.
The autocorrelation function of the heat flux of WCA potential and LJ potential is shown below.

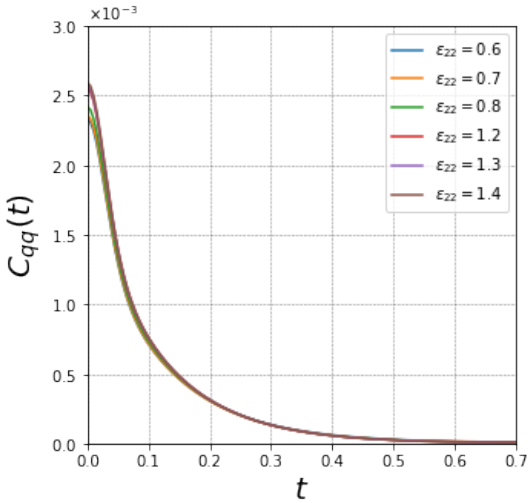

Figure 3.23: C_{qq} for WCA potential with various ε_{22} values

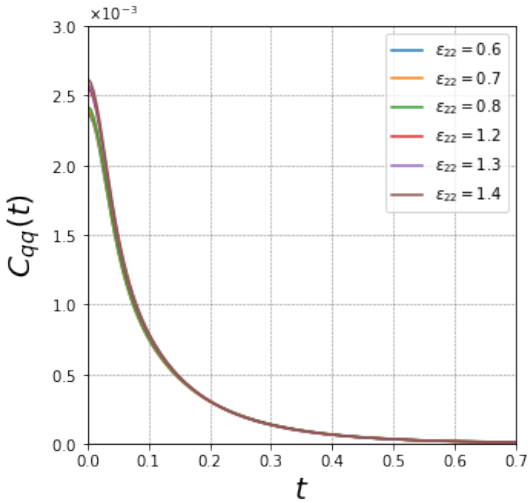

Figure 3.24: C_{qq} for LJ potential with various ε_{22} values

Changes in ε_{22} do not change the relaxation time of the heat flux correlation function, whether there are attractive or not. From the results shown in C_{qq} and using the Green-Kubo formula defined eq. (2.53), we calculate the transport coefficients of the heat flux.

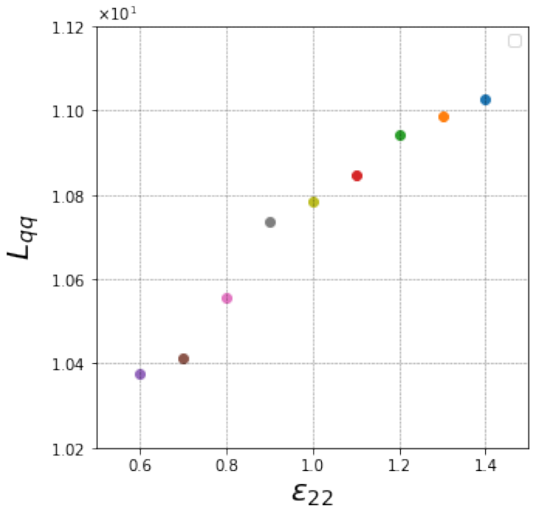

Figure 3.25: L_{qq} for WCA potential with various ε_{22} values

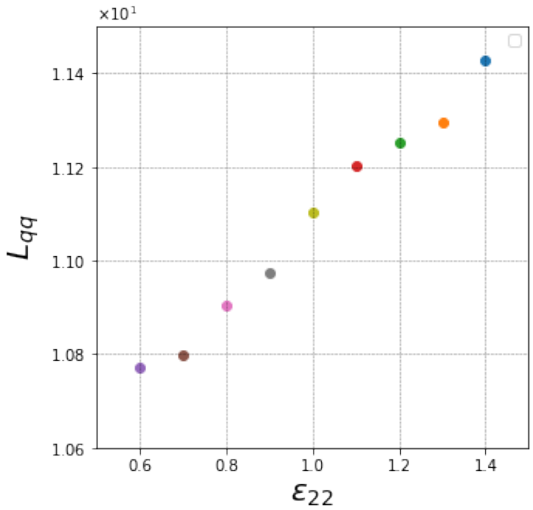

Figure 3.26: L_{qq} for LJ potential with various ε_{22} values

The heat transport coefficient increased as the value of ε_{22} increased. There no defference in each potentials.

3.2.2 Mass autocorrelatin function

By using equation eq. (2.40), we calculate the mass flux $\boldsymbol{J}_1$ and the autocorrelation function of the mass flux C_{11} of WCA potential and LJ potential is shown below.

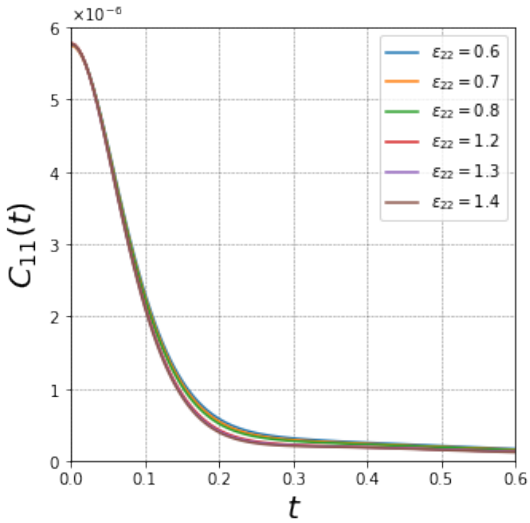

Figure 3.27: C_{11} for WCA potential with various ε_{22} values

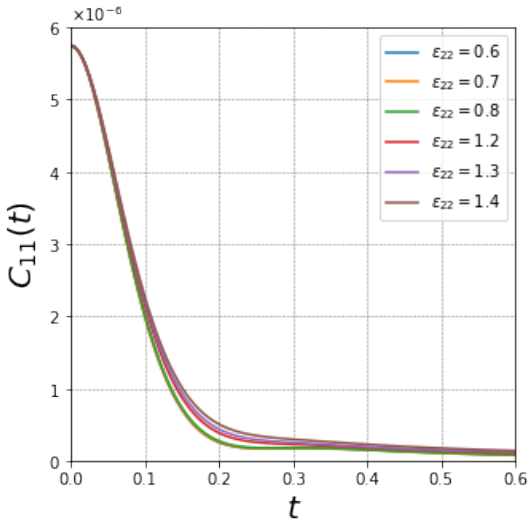

Figure 3.28: C_{11} for LJ potential with various ε_{22} values

Relaxation time does not change for either potential, but ε_{22} dependence changes in each potential.

From the results shown in C_{11} and by using the Green-Kubo formula eq. (2.54), we calculate the transport coefficients of mass flux L_{11}.

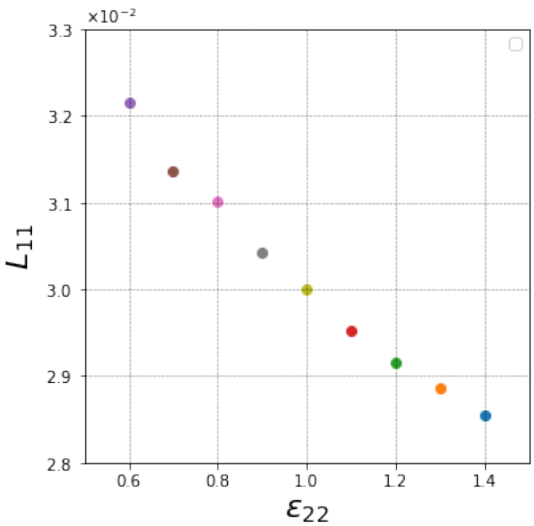

Figure 3.29: L_{11} for WCA potential with various ε_{22} values

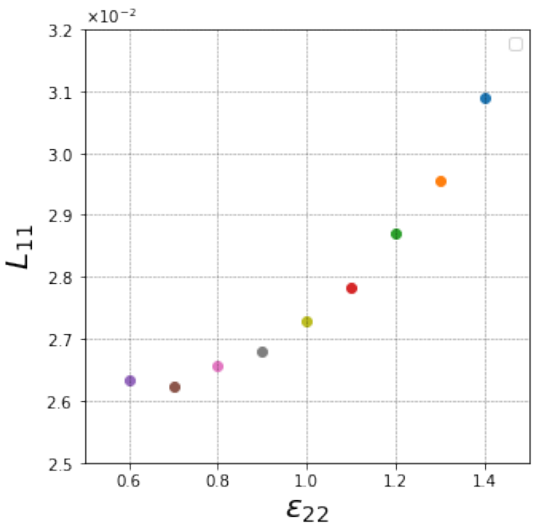

Figure 3.30: L_{11} for LJ potential with various ε_{22} values

In the WCA potential, the value of L_{11} increases as ε_{22} increases. On the other hand, in the LJ potential, the dependence is reversed.

3.2.3 Mass and heat crosscorrelation function

By using equation eq. (2.40) and eq. (2.39),we calculate mass and heat crosscorrelation function of the fluxes C_{1q}.

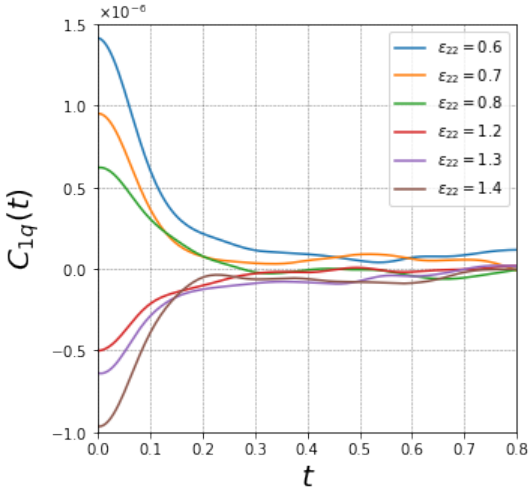

Figure 3.31: C_{1q} for WCA potential with various ε_{22} values

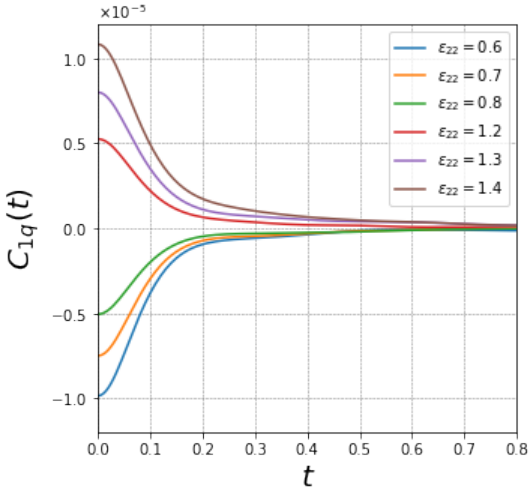

Figure 3.32: C_{1q} for LJ potential with various ε_{22} values

No contribution of vibration was seen in either potential, and the value decreased monotonically from the value at time $t = 0$. We can see the fluctuations in WCA potential, but we can not see in the LJ potential because LJ potential have long cutoff distance and particles are influenced by around the particles. From the results in C_{1q} and by using the Green-Kubo formula shown in eq. (2.55), we calculate mass and heat cross transport coefficients L_{1q}.

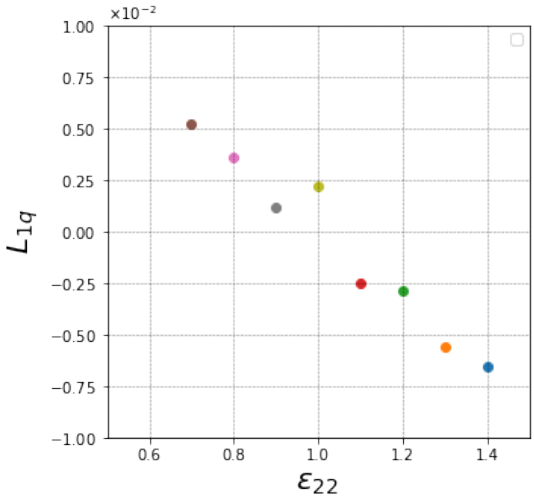

Figure 3.33: L_{1q} for WCA potential with various ε_{22} values

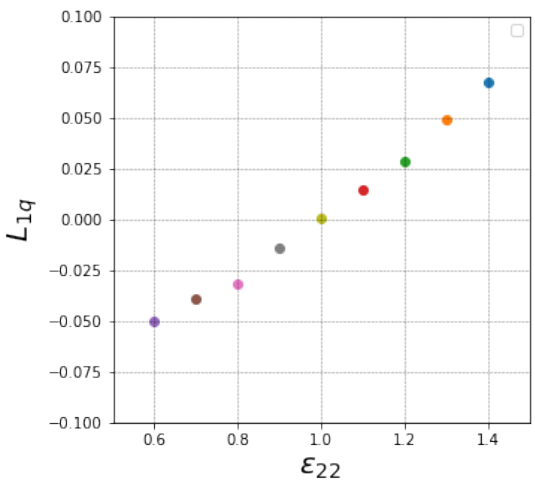

Figure 3.34: L_{1q} for LJ potential with various ε_{22} values

When $\varepsilon_{22} = 1$, L1q becomes 0 due to symmetry. However, it was found that the sign of L_{1q} becomes negative when $\varepsilon_{22} > 1$ and positive when$\varepsilon_{22} < 1$ On the other hand, in the LJ potential, the sign of L_{1q} becomes positibve $\varepsilon_{22} > 0$.

3.2.4 Radial distrobution function

To check if the structure has changed due to the difference in potential, we calculate radial distribution function(rdf) (eq. (2.70)) in each systems.

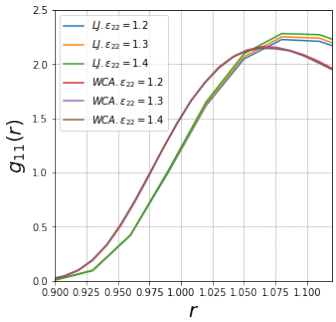

Figure 3.35: rdf of between particles 1 1

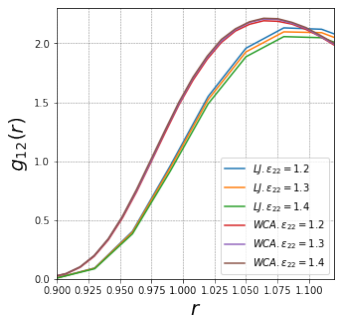

Figure 3.36: rdf of between particles 1 2

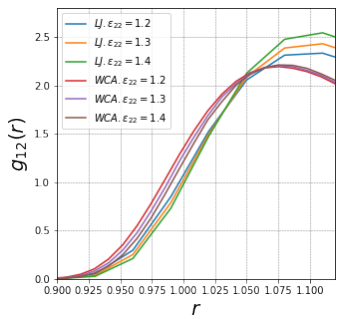

Figure 3.37: rdf of between particles 2 2

The first peak of WCA potential is closer than the first peak of LJ potential. The difference of potential parameter ε_{22} is different in each potential. In case of WCA potential, There are no difference of the first peak but there are differences of the distance that is closer than the fist peak. On the other hand. LJ potetial has difference at the first peak. It differences may affect the change of transport coefficients.

3.2.5 Mean square displacement

When ε_{22} is 1.3, we calculate mean square displacement by using eq. (2.71) to check if the diffusion has changed due to the difference in potential.

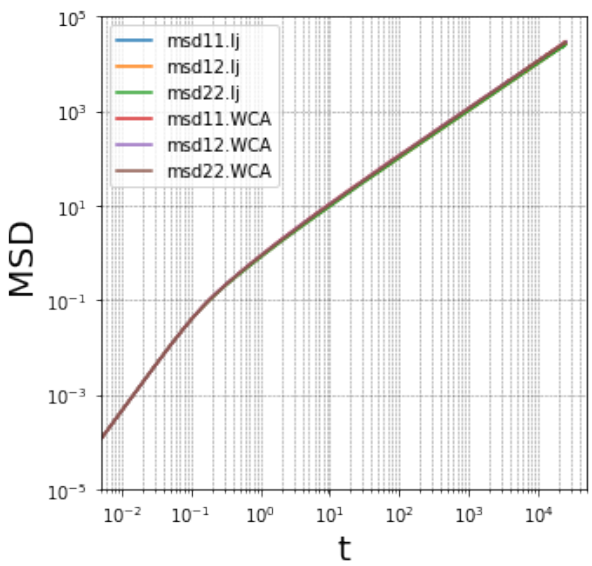

Figure 3.38: Mean square displacement when ε_{22} is 1.3

We can see there are no diifference in each potential because diffusion depends on mainly repulsive forces. If we change the potential parameter ε_{22}, we can not see the case effect.

3.2.6 Discussion

When the simulation was performed using the potential parameter(ε_{22}) of particle 2 as a parameter while keeping the potential parameter(ε_{22}) of particle 1 at 1.0, it was found that the ε_{22} dependence of the cross-transportation coefficient differs between the WCA potential and the LJ potential. This revealed that the presence or absence of attractive force reverses the ε_{22} dependence of the transport coefficient. However, by Reith et al[18], they reported the Soret coefficients of species with deeper potential wells prefer the cold side of the simulation box. They considered that the species with the lower mobility favors the cold side. I don't the directly reason why our results and previous research is different result. However I think this contradiction is governed by difference of set of temperature and our heat definition. Reith et al sets temperature 0.8, However we sets temperature 1.5.

To understand which energy flux is more important factor, we decompose heat flux into kinetic part and potential part. By using the equation eq. (2.40), eq. (2.39) and eq. (3.4),we calculate mass and heat crosscorrelation function of kinetic part in each potentials.

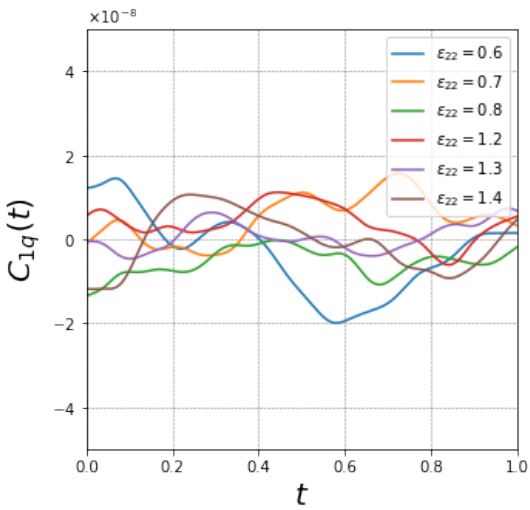

Figure 3.39: C_{1q} for WCA potential of kinetic part with various ε_{22} values

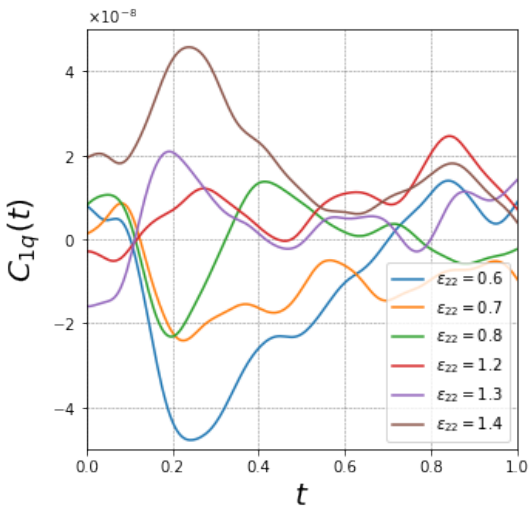

Figure 3.40: C_{1q} for LJ potential of potential part with various ε_{22} values

We found that mass and heat crosscorrelation function of kinetic part has order 10^{-8}, so we can ignore the effect of kinetic part. As a result, we found that the difference of mass and heat crosscorrelation function is due to the potential part.

3.2.7 Conclusion

In this section, we investigate potential parameter(ε_{22}) dependence of transport coefficient in each potentials. We summary the result in this section.

Purpose :
investigate the ε_{22} dependence of transport coefficient in each potentials

Result of WCA potential :
that particles with deeper potential move to the lower temperature side and that particles with shallower potential move to the higher temperature side

Result of LJ potential :
that particles with deeper potential move to the higher temperature side and that particles with shallower potential move to the lower temperature side

Consideration of rdf :
the first peak of WCA potential is closer than the first peak of LJ potential and the distance influenced by ε_{22} is differed.

Consideration of MSD :
There are almost no difference in each potential.

Discussion :
we found that the difference of mass and heat crosscorrelation function is due to the potential part.

3.3 Temperature dependence

We calculate the C_{11}, the C_{qq} and the C_{1q} with varying M. We performed the simulation set C.

3.3.1 Heat autocorrelation function

By using equation eq. (2.39) and the Green-Kubo formula eq. (2.53), we calculate heat flux.
The heat autocorrelation function for LJ potential is shown below.

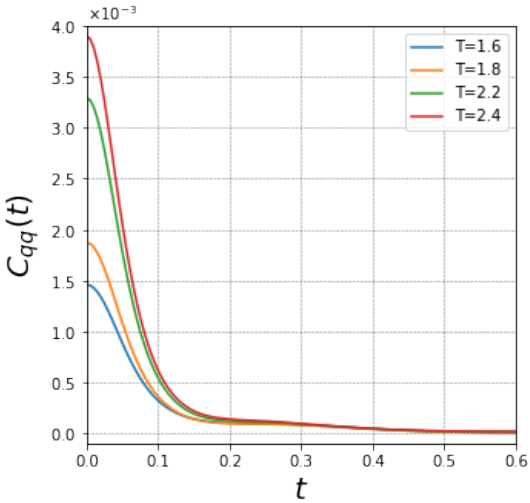

Figure 3.41: C_{qq} for LJ potential with various T values

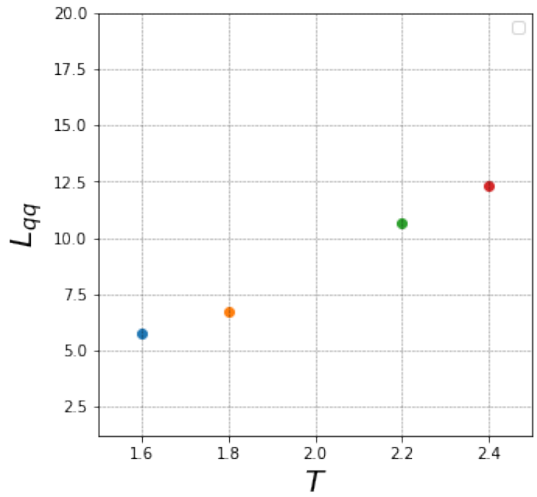

Figure 3.42: L_{qq} for LJ potential with various T values

We can see the heat autocorrelaation function at $t = 0$ is increased because the velocity is faster. As a result, the heat transport coefficient is increased as the temperature is increased.

3.3.2 Mass autocorrelation function

By using equation eq. (2.40) and the Green-Kubo formula eq. (2.54), we calculate mass flux.
The mass autocorrelation function for LJ potential is shown below.

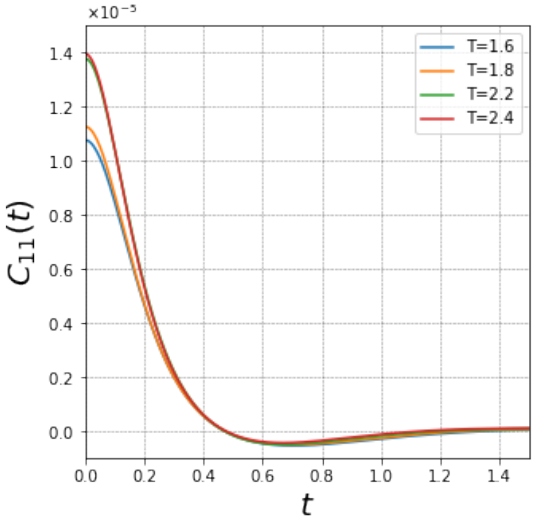

Figure 3.43: C_{11} for LJ potential with various T values

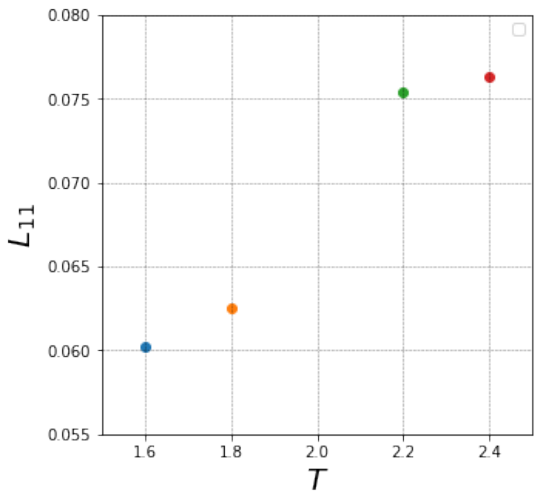

Figure 3.44: L_{11} for LJ potential with various T values

We can see the mass autocorrelaation function at $t = 0$ is increased because the velocity is faster. As a result, the mass transport coefficient is increased as the temperature is increased.

3.3.3 Heat and mass crosscorrelation function

By using equation eq. (2.40) , eq. (2.39) and the Green-Kubo formula eq. (2.55), we calculate heat flux.
The heat and mass crosscorrelation function for LJ potential is shown below.

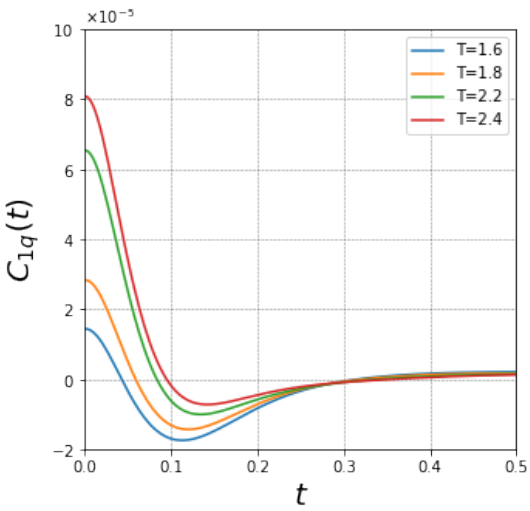

Figure 3.45: C_{1q} for LJ potential with various T values

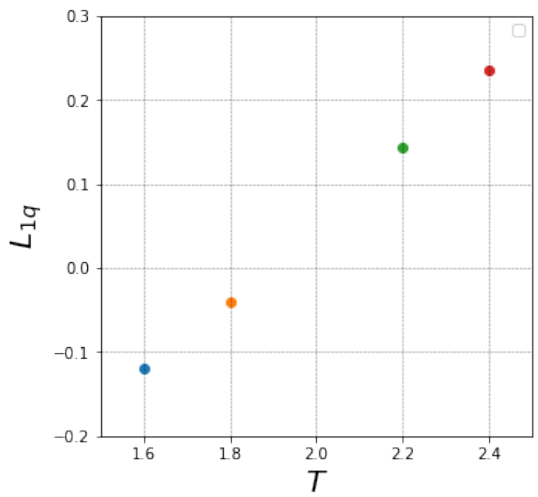

Figure 3.46: L_{1q} for LJ potential with various T values

We can see the sign of transport coefficients is changed when the temperature is increased.

3.3.4 Discussion

When we changed the temperature as a parameter while keeping the mass of particle 2 at 16.0, we found that the cross transport coefficients depend on the temperature. We can see the sign change of the heat and mass cross transport coefficients as the temperature is increased. To understand the change, we decompose the heat flux into the kinetic part and the potential part.

By using eq. (2.40), eq. (2.39), eq. (3.5), eq. (3.4), we calculate mass and heat crosscorrelation function of kinetic part in each potentials.

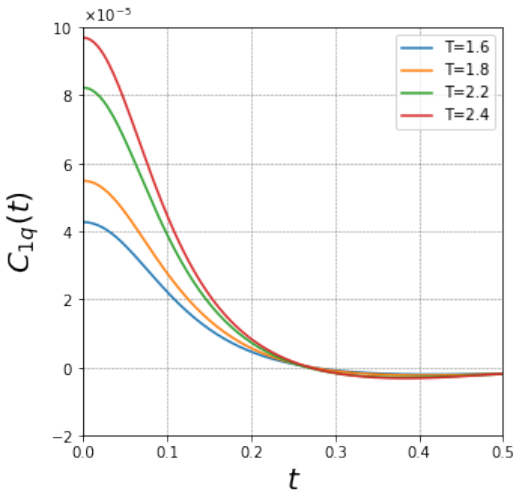

Figure 3.47: C_{1q} of kinetic part for LJ potential with various T values

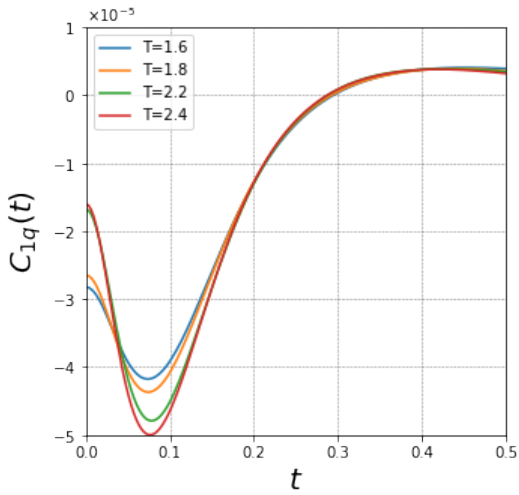

Figure 3.48: C_{1q} of potential part for LJ potential with various T values

We found that the transport of kinetic part is increased due to the increase of velocity. We found that the potential part has a bigger oscillatory damp as the temperature is increased. I thought that the change of behavior is due to the potential part because the collisions more important than attractive force when we change the temperature. However, that idea was not true. The change of behavior is due to the increase of the kinetic part.

3.3.5 Conclusion

In this section, we investigate temperature dependence of transport coefficient. We summary the result in this section.

Purpose :

investigate the temperature dependence of transport coefficients

Result :

When the temperature is lower than 2.0, that particles with lighter mass move to the higher temperature side and that particles with heavier mass move to the lower temperature side. When the temperature is lower than 2.0, that particles with heavier mass move to the higher temperature side and that particles with lighter mass move to the lower temperature side.

Discussion :

The change of behavior is due to the increase of the kinetic part.

Chapter 4

Conclusions

We found that, when the symmetry of the system is held, the cross transport coefficients is zero. Meanwhile, even for the WCA potential, which solely generates a repulsive force, the cross transport coefficient is not 0 when the symmetry is broken.

We found that LJ potential and WCA potential exhibited different behavior due to the attractive force and the attractive force plays an important role for the cross transport coefficient. We also found that in a high temperature, the cross transport coefficient is insensitive to the difference of the interaction potential.

Chapter 5

Appendix

5.1 Momentum autocorrelation function

5.1.1 No constraint conditions

No restraint conditions, the momentum autocorrelation function at $t = 0$ can be theoretically analyzed. First, we determine a normalized constant (A). Since the probability distribution function of each momentum follows the Boltzmann distribution function, the probability distribution function of $\boldsymbol{P}_1$ is defined as

$$P(\boldsymbol{P}_1) = \int_{-\infty}^{\infty} A \exp(-\frac{\boldsymbol{P}_1^2}{2N_1 m k_B T}) \exp(-\frac{\boldsymbol{P}_2^2}{2N_2 M k_B T}) d\boldsymbol{P}_2 \tag{5.1}$$

$$= \left(\sqrt{2k_B T \pi M N_2}\right)^{3/2} A \exp(-\frac{\boldsymbol{P}_2^2}{2N_2 M k_B T}). \tag{5.2}$$

Therefore normalized constant A is

$$1 = \int_{-\infty}^{\infty} \left(\sqrt{\frac{1}{2k_B T \pi M N_2}}\right)^3 A \exp(-\frac{\boldsymbol{P}_2^2}{2N_2 M k_B T}) d\boldsymbol{P}_1 \tag{5.3}$$

$$A = \left(\sqrt{4k_B^2 T^2 \pi^2 m M N_1 N_2}\right)^3. \tag{5.4}$$

By using the normalized constant A, the momentum autocorrelation function at $t = 0$ is theoretically derived

$$\begin{aligned}
\langle \boldsymbol{P}_1(0) \boldsymbol{P}_1(0) \rangle &= \left(\sqrt{\frac{1}{4k_B^2 T^2 \pi^2 m M N_1 N_2}}\right)^3 \int_{-\infty}^{\infty} \boldsymbol{P}_1^2(0) \exp(-\frac{\boldsymbol{P}_1^2}{2N_1 m k_B T}) \exp(-\frac{\boldsymbol{P}_2^2}{2N_2 M k_B T}) d\boldsymbol{P}_1 \boldsymbol{P}_2 \\
&= \left(\sqrt{\frac{1}{2k_B T \pi m N_1}}\right)^3 \int_{-\infty}^{\infty} \boldsymbol{P}_1^2(0) \exp(-\frac{\boldsymbol{P}_1^2}{2N_1 m k_B T}) d\boldsymbol{P}_1 \\
&= 3N_1 m k_B T. \qquad (5.5)
\end{aligned}$$

5.1.2 Under constraint conditions

Theoretical calculation is performed under the constraint condition that the total momentum is 0 for the entire system. Since the probability distribution function of each momentum follows the Boltzmann distribution function,the probability distribution function of $\boldsymbol{P}_1$ is defined as

$$P(\boldsymbol{P}_1) = \int_{-\infty}^{\infty} A\delta(\boldsymbol{P}_1+\boldsymbol{P}_2)\exp(-\frac{\boldsymbol{P}_1^2}{2N_1mk_BT})\exp(-\frac{\boldsymbol{P}_2^2}{2N_2Mk_BT})d\boldsymbol{P}_2 \tag{5.6}$$

$$= A\exp(-\frac{\boldsymbol{P}_1^2}{2N_1mk_BT})\exp(-\frac{\boldsymbol{P}_1^2}{2N_2Mk_BT}). \tag{5.7}$$

Therefore normalized constant A is

$$1 = \int_{-\infty}^{\infty} A\exp(-\frac{(N_1m+N_2M)\boldsymbol{P}_2^2}{2N_1N_2mMk_BT})d\boldsymbol{P}_1 \tag{5.8}$$

$$A = \left(\frac{1}{\sqrt{2\pi}}\sqrt{\frac{N_1m+N_2M}{k_BTmMN_1N_2}}\right)^3. \tag{5.9}$$

By using the normalized constant A, the momentum autocorrelation function at $t=0$ is theoretically derived

$$\left(\frac{1}{\sqrt{2\pi}}\sqrt{\frac{N_1m+N_2M}{k_BTmMN_1N_2}}\right)^3 \int_{-\infty}^{\infty} \boldsymbol{P}_1^2(0)\delta(\boldsymbol{P}_1+\boldsymbol{P}_2)\exp(-\frac{\boldsymbol{P}_1^2}{2N_1mk_BT})\exp(-\frac{\boldsymbol{P}_2^2}{2N_2Mk_BT})d\boldsymbol{P}_1\boldsymbol{P}_2$$

$$= \left(\frac{1}{2\pi}\right)^3\left(\frac{1}{\sqrt{2\pi}}\sqrt{\frac{N_1m+N_2M}{k_BTmMN_1N_2}}\right)^3 \int_{-\infty}^{\infty} \boldsymbol{P}_1^2(0)\exp(-i\boldsymbol{k}\cdot(\boldsymbol{P}_i+\boldsymbol{P}_j))\exp(-\frac{\boldsymbol{P}_1^2}{2N_1mk_BT})\exp(-\frac{\boldsymbol{P}_2^2}{2N_2Mk_BT})d\boldsymbol{P}_1\boldsymbol{P}_2d\boldsymbol{k}$$

$$= \left(\frac{1}{2\pi}\right)^3\left(\frac{1}{\sqrt{2\pi}}\sqrt{\frac{N_1m+N_2M}{k_BTmMN_1N_2}}\right)^3\left(\sqrt{2N_2MK_BT}\right)^3$$

$$\int_{-\infty}^{\infty}\int_{-\infty}^{\infty} \boldsymbol{P}_1^2(0)\exp(-\frac{1}{2N_1mk_BT}(\boldsymbol{P}_1+N_1mk_BTi\boldsymbol{k})^2)\exp(-\frac{(N_1m+N_2M)k_BT\boldsymbol{k}^2}{2})d\boldsymbol{P}_1d\boldsymbol{k}.$$

where we rewrite the delta function using the inverse Fourier transform relation

$$\delta(\boldsymbol{P}_1+\boldsymbol{P}_2) = \left(\frac{1}{2\pi}\right)^3\int_{-\infty}^{\infty}\exp(-i\boldsymbol{k}\cdot(\boldsymbol{P}_i+\boldsymbol{P}_j))d\boldsymbol{k}. \tag{5.10}$$

then we perform change of variables ($\boldsymbol{q}_i = \boldsymbol{P}_1 + N_1mk_BTi\boldsymbol{k}$)

$$= \left(\frac{1}{2\pi}\right)^3\left(\frac{1}{\sqrt{2\pi}}\sqrt{\frac{N_1m+N_2M}{k_BTmMN_1N_2}}\right)^3\left(\sqrt{2N_2Mk_BT}\right)^3$$

$$\int_{-\infty}^{\infty}\int_{-\infty}^{\infty}(\boldsymbol{q}_1-N_1mk_BTi\boldsymbol{k})^2\exp(-\frac{q_1^2}{2N_1mk_BT})\exp(-\frac{(N_1m+N_2M)k_BT\boldsymbol{k}^2}{2})d\boldsymbol{q}_1d\boldsymbol{k}$$

$$= 3mN_1k_BT\left(\frac{N_2M}{N_1m+N_2M}\right). \tag{5.11}$$

5.1.3 Comparison between simulation and theory

Now, we compare simulation result and theory when time is 0.

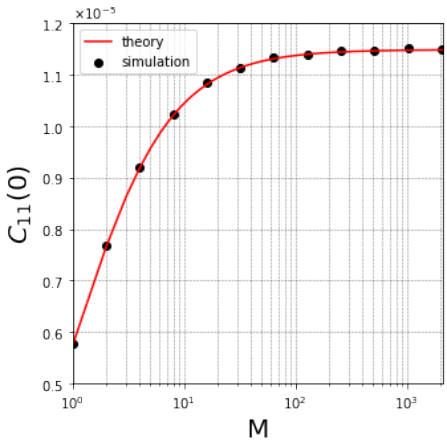

Figure 5.1: WCA.mass autocorrelation

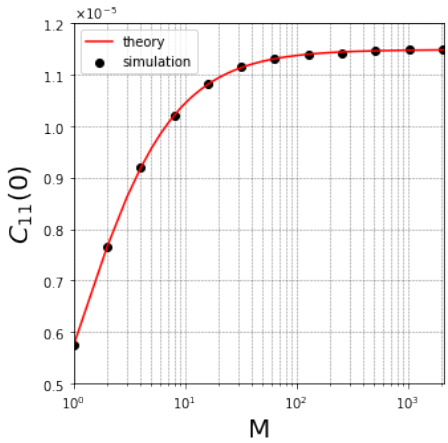

Figure 5.2: lj.mass autocorrelation

The theoretical result and the simulation result are consistent in each potential. we can confirm the mass autocorrelation function at $t = 0$ has dependence on mass.

5.2 Mass and heat crosscorrelation function

5.2.1 No constraint conditions

No restraint conditions, the mass and heat crosscorrelation function at $t = 0$ can be theoretically analyzed if we assume a rigid body collision in the dilute gas. First, we determine normalized constant (A). Since the probability distribution function of each velocity follows the Boltzmann distribution function,the probability distribution function of velocity of i particle $\boldsymbol{v}_i$ is defined as

$$\begin{aligned} p(v_i) &= \int_{-\infty}^{\infty} A \exp(-\sum_i \frac{mv_i^2}{2k_BT}) \exp(-\sum_j \frac{Mv_j^2}{2k_BT}) dv_j \\ &= \left(\sqrt{\frac{2k_BT\pi}{M}}\right)^N A \exp(-\sum_i \frac{mv_i^2}{2k_BT}). \end{aligned} \tag{5.12}$$

Therefore normalized constant A is

$$\begin{aligned} 1 &= \int_{-\infty}^{\infty} \left(\sqrt{\frac{2k_BT\pi}{M}}\right)^N A \exp(-\sum_i \frac{mv_i^2}{2k_BT}) dv_i \\ A &= \left(\sqrt{\frac{mM}{4k_B^2T^2\pi^2}}\right)^N. \end{aligned} \tag{5.13}$$

By using normalized constant A, the mass and heat crosscorrelation function at $t = 0$ is theoretically derived

$$\begin{aligned} \langle \boldsymbol{P}_1(0)\boldsymbol{J}_q(0)\rangle &= \left(\sqrt{\frac{mM}{4k_B^2T^2\pi^2}}\right)^N \int_{-\infty}^{\infty}\int_{-\infty}^{\infty} \sum_i^N mv_i \left(\sum_i^N \frac{mv_i^2}{2} v_i + \sum_j^N \frac{Mv_j^2}{2} v_j\right) \exp(-\sum_i \frac{mv_i^2}{2k_BT}) \exp(-\sum_j \frac{Mv_j^2}{2k_BT}) dv_i dv_j \\ &= \left(\sqrt{\frac{mM}{4k_B^2T^2\pi^2}}\right)^N \left(\frac{1}{2}\right) \int_{-\infty}^{\infty}\int_{-\infty}^{\infty} \left(\sum_i^N m^2 v_i^4\right) \exp(-\sum_i \frac{mv_i^2}{2k_BT}) \exp(-\sum_j \frac{Mv_j^2}{2k_BT}) dv_i dv_j \\ &= \left(\sqrt{\frac{m}{2k_BT\pi}}\right)^N \left(\frac{1}{2}\right) \int_{-\infty}^{\infty} \left(\sum_i^N m^2 v_i^4\right) \exp(-\sum_i \frac{mv_i^2}{2k_BT}) dv_i \\ &= \left(\sqrt{\frac{m}{2k_BT\pi}}\right)^N \left(\frac{1}{2}\right) \frac{N}{2} m^2 \left(\frac{2k_BT}{m}\right)^{N/2+2} \\ &= \frac{3}{2} N (k_BT)^2. \end{aligned} \tag{5.14}$$

5.2.2 Under constraint conditions

Theoretical calculation is performed under the constraint condition that the total momentum is 0 for the entire system. Mass and heat crosscorrelation function at $t = 0$ can be theoretically analyzed if we assume a rigid body collision in the dilute gas. First, we determine normalized constant (A) Since the probability distribution function of each velocity follows the Boltzmann distribution function,the probability distribution function of velocity of i particle $\boldsymbol{v}_i$ is defined as

$$\begin{aligned}
p(v_i) &= \int_{-\infty}^{\infty} A\delta(\sum_i^{N_1} mv_i + \sum_j^{N_2} Mv_j)\exp(-\sum_i \frac{mv_i^2}{2k_BT})\exp(-\sum_j \frac{Mv_j^2}{2k_BT})dv_j \\
&= \int_{-\infty}^{\infty}\int_{-\infty}^{\infty} A\exp(-ik(\sum_i^{N_1} mv_i + \sum_j^{N_2} Mv_j))\exp(-\sum_i \frac{mv_i^2}{2k_BT})\exp(-\sum_j \frac{Mv_j^2}{2k_BT})dv_j dk \\
&= \left(\sqrt{\frac{2\pi}{N(m+M)k_BT}}\right)\left(\sqrt{\frac{2k_BT\pi}{M}}\right)^N A\exp(-\sum_i \frac{mv_i^2}{2k_BT}).
\end{aligned} \tag{5.15}$$

For simplification,we calculate as $N = N_1 = N_2$.therefore normalized constant A is

$$\begin{aligned}
1 &= \int_{-\infty}^{\infty}\left(\sqrt{\frac{2\pi}{N(m+M)k_BT}}\right)\left(\sqrt{\frac{2k_BT\pi}{M}}\right)^N A\exp(-\sum_i \frac{mv_i^2}{2k_BT})dv_i \\
A &= \left(\sqrt{\frac{N(m+M)k_BT}{2\pi}}\right)\left(\sqrt{\frac{m}{2k_BT\pi}}\right)^N\left(\sqrt{\frac{M}{2k_BT\pi}}\right)^N.
\end{aligned} \tag{5.16}$$

By using normalized constant A, the mass and heat crosscorrelation function at $t = 0$ is theoretically derived

$$\begin{aligned}
&\langle \boldsymbol{P}_1(0)\boldsymbol{J}_q(0)\rangle = \left(\sqrt{\frac{N(m+M)k_BT}{2\pi}}\right)\left(\sqrt{\frac{m}{2k_BT\pi}}\right)^N\left(\sqrt{\frac{M}{2k_BT\pi}}\right)^N \\
&\int_{-\infty}^{\infty}\int_{-\infty}^{\infty}\sum_i^N mv_i\left(\sum_i^N \frac{mv_i^2}{2}v_i + \sum_j^N \frac{Mv_j^2}{2}v_j\right)\delta(\sum_i^N mv_i + \sum_j^N Mv_j)\exp(-\sum_i \frac{mv_i^2}{2k_BT})\exp(-\sum_j \frac{Mv_j^2}{2k_BT})dv_i dv_j \\
&= \left(\sqrt{\frac{N(m+M)k_BT}{2\pi}}\right)\left(\sqrt{\frac{m}{2k_BT\pi}}\right)^N\left(\sqrt{\frac{M}{2k_BT\pi}}\right)^N\int_{-\infty}^{\infty}\int_{-\infty}^{\infty}\int_{-\infty}^{\infty}\sum_i^N mv_i\left(\sum_i^N \frac{mv_i^2}{2}v_i + \sum_j^N \frac{Mv_j^2}{2}v_j\right) \\
&\exp(-ik(\sum_i^N mv_i + \sum_j^N Mv_j))\exp(-\sum_i \frac{mv_i^2}{2k_BT})\exp(-\sum_j \frac{Mv_j^2}{2k_BT})dv_i dv_j dk \\
&= \left(\frac{1}{2}\right)\left(\sqrt{\frac{N(m+M)k_BT}{2\pi}}\right)\left(\sqrt{\frac{m}{2k_BT\pi}}\right)^N\left(\sqrt{\frac{M}{2k_BT\pi}}\right)^N\int_{-\infty}^{\infty}\int_{-\infty}^{\infty}(\sum_i^N m^2v_i^4 + \sum_{ik} m^2v_iv_k^3 + \sum_i^N mv_i\sum_j^N Mv_j^2v_j) \\
&\exp(-ik(\sum_i^N mv_i + \sum_j^N Mv_j))\exp(-\sum_i \frac{mv_i^2}{2k_BT})\exp(-\sum_j \frac{Mv_j^2}{2k_BT})dv_i dv_j dk \\
&= \left(\frac{1}{2}\right)\left(\sqrt{\frac{N(m+M)k_BT}{2\pi}}\right)\left(\sqrt{\frac{m}{2k_BT\pi}}\right)^N\left(\sqrt{\frac{M}{2k_BT\pi}}\right)^N\int_{-\infty}^{\infty}\int_{-\infty}^{\infty}\int_{-\infty}^{\infty}(\sum_i^N m^2v_i^4 + \sum_{ik} m^2v_iv_k^3 + \sum_i^N mv_i\sum_j^N Mv_j^2v_j) \\
&\exp(-\sum_i \frac{m}{2k_BT}(v_i + k_BTik)^2)\exp(-\sum_j \frac{M}{2k_BT}(v_j + k_BTik)^2)\exp(-\sum_i \frac{mk_BTk^2}{2})\exp(-\sum_i \frac{Mk_BTk^2}{2})dv_i dv_j dk.
\end{aligned} \tag{5.17}$$

We perform change of variables $q_i = v_i + k_B Tik$、$q_j = v_j + k_B Tik$

$$\langle P_1(0)J_q(0)\rangle = \left(\frac{1}{2}\right)\left(\sqrt{\frac{N(m+M)k_BT}{2\pi}}\right)\left(\sqrt{\frac{m}{2k_BT\pi}}\right)^N\left(\sqrt{\frac{M}{2k_BT\pi}}\right)^N$$
$$\int_{-\infty}^{\infty}\int_{-\infty}^{\infty}\int_{-\infty}^{\infty}(\sum_i^N m^2(q_i-k_BTik)^4+\sum_{ik}m^2(q_i-k_BTik)(q_k-k_BTik)^3+mM\sum_i^N\sum_j^N(q_i-k_BTik)(q_j-k_BTik)^3)$$
$$\exp(-\sum_i\frac{mq_i^2}{2k_BT})\exp(-\sum_j\frac{Mq_j^2}{2k_BT})\exp(-\sum_i\frac{mk_BTk^2}{2})\exp(-\sum_i\frac{Mk_BTk^2}{2})dv_idv_jdk$$
$$=\left(\frac{1}{2}\right)\left(\sqrt{\frac{N(m+M)k_BT}{2\pi}}\right)\left(\sqrt{\frac{m}{2k_BT\pi}}\right)^N\left(\sqrt{\frac{M}{2k_BT\pi}}\right)^N\int_{-\infty}^{\infty}\int_{-\infty}^{\infty}\int_{-\infty}^{\infty}$$
$$(\sum_i^N m^2(q_i^4-6k_B^2T^2k^2q_i^2+(k_BTk)^4$$
$$+\sum_{ik}m^2(q_i-k_BTik)(q_k^3-3k_BTikq_k^2-3(k_BTk)^2q_k+i(k_BTk)^3)$$
$$+mM\sum_i^N\sum_j^N(q_i-k_BTik)(q_j^3-3k_BTikq_j^2-3(k_BTk)^2q_j+i(k_BTk)^3)$$
$$\exp(-\sum_i\frac{mq_i^2}{2k_BT})\exp(-\sum_j\frac{Mq_j^2}{2k_BT})\exp(-\sum_i\frac{mk_BTk^2}{2})\exp(-\sum_i\frac{Mk_BTk^2}{2})dv_idv_jdk. \tag{5.18}$$

We perform Gauss integrals

$$=\left(\frac{1}{2}\right)\left(\sqrt{\frac{N(m+M)k_BT}{2}}\right)m^2(\left(\frac{3N}{4}\right)\left(\frac{2k_BT}{m}\right)^{+2}\left(\frac{2}{(m+M)Nk_BT}\right)^{1/2}$$
$$-\left(\frac{N}{2}\right)\frac{1}{2}6k_B^2T^2\left(\frac{2}{(m+M)Nk_BT}\right)^{3/2}\left(\frac{2k_BT}{m}\right)^{+1}+\left(\frac{3}{4}\right)(k_BT)^4\left(\frac{2}{(m+M)Nk_BT}\right)^{5/2})$$
$$+m^2(-3k_B^2T^2\left(\frac{N}{2}\right)\frac{1}{2}\left(\frac{2}{(m+M)Nk_BT}\right)^{3/2}\left(\frac{2k_BT}{m}\right)^{+1}+(\left(\frac{3}{4}\right)(k_BT)^4\left(\frac{2}{(m+M)Nk_BT}\right)^{5/2})$$
$$+mM(-3k_B^2T^2\left(\frac{N}{2}\right)\frac{1}{2}\left(\frac{2}{(m+M)Nk_BT}\right)^{3/2}\left(\frac{2k_BT}{M}\right)^{+1}+(\left(\frac{3}{4}\right)\left(\frac{2}{(m+M)Nk_BT}\right)^{5/2}(k_BT)^4))$$
$$=\frac{3}{2}N(k_BT)^2(1-4\left(\frac{m}{N(m+M)}\right)+\frac{m(2m+M)}{4N}\left(\frac{1}{(m+M)N}\right)^2). \tag{5.19}$$

5.3 Transport coefficient in gas

We now consider a binary mixture in which both the temperature and the composition vary in the z direction. If the pressure is uniform. species has flux of thermal motions of the molecules and mass motion which is necessary to maintain uniformity of pressure.

In a gas in which the velocity distribution function is Maxwellian, the number of molecules impinging on unit area moving with the mean velocity is $\frac{1}{4}n\bar{C}_1$,where n is the number density and $\bar{C}$ is the mean thermal velocity. And we define two variables,$\bar{z}_1$ and $\bar{z}'_1$, which is distance to transfer number and mean speed. Thus we refer to the plane $z = 0$ the flux of molecules in the negative z direction

$$\frac{1}{4}\left(n_1^0 + \frac{\partial n_1}{\partial z}\bar{z}_1\right)\left(\bar{C}_1^0 + \frac{\partial \bar{C}}{\partial z}\bar{z'}_1\right). \tag{5.20}$$

The flux of molecules in the positive z direction

$$\frac{1}{4}\left(n_1^0 - \frac{\partial n_1}{\partial z}\bar{z}_1\right)\left(\bar{C}_1^0 - \frac{\partial \bar{C}}{\partial z}\bar{z'}_1\right). \tag{5.21}$$

As a result, the net flux of particle 1 in the positive direction is

$$\Gamma'_1 = -\frac{1}{2}\left[\frac{\partial n_1}{\partial z}\bar{z}_1\bar{C}_1 + \frac{\partial \bar{C}_1}{\partial z}\bar{z'}_1 n_1\right]. \tag{5.22}$$

Similarly,the net flux of particle 2 in the positive direction is

$$\Gamma'_2 = -\frac{1}{2}\left[\frac{\partial n_2}{\partial z}\bar{z}_2\bar{C}_2 + \frac{\partial \bar{C}_2}{\partial z}\bar{z'}_2 n_2\right]. \tag{5.23}$$

The diffusion velocity is

$$\bar{c}_1 - \bar{c}_2 = \frac{\Gamma_1}{n_1} - \frac{\Gamma_2}{n_2} = -\frac{1}{2}\left[\frac{1}{n_1}\frac{\partial n_1}{\partial z}\bar{z}_1\bar{C}_1 - \frac{1}{n_2}\frac{\partial n_2}{\partial z}\bar{z}_2\bar{C}_2 + \frac{\partial \bar{C}_1}{\partial z}\bar{z'}_1 - \frac{\partial \bar{C}_2}{\partial z}\bar{z'}_2\right], \tag{5.24}$$

where $\frac{\Gamma_1}{n_1} = \bar{c}_1$ and $\frac{\Gamma_2}{n_2} = \bar{c}_2$. By using partial pressure is p, p is satisfy

$$n_{10}p = n_1 kT. \tag{5.25}$$

Derivative of above equation,we see

$$\frac{\partial n_1}{\partial z} = \frac{p}{k}\left[\frac{1}{T}\frac{\partial n_{10}}{\partial z} - \frac{n_{10}}{T^2}\frac{\partial T}{\partial z}\right]. \tag{5.26}$$

Now we assume that we can neglect the distribution between the mean velocity and root-mean-square

$$\bar{C} = \left(\frac{3kT}{m}\right)^{1/2}. \tag{5.27}$$

$$\frac{\partial \bar{C}_1}{\partial z} = \left(\frac{3k}{m}\right)^{1/2}\frac{1}{2T^{1/2}}\frac{\partial T}{\partial z}. \tag{5.28}$$

We use above two equation, we get

$$\begin{aligned}\frac{1}{n_1}\frac{\partial n_1}{\partial z}\bar{C}_1\bar{z}_1 &= \frac{p}{k}\left(\frac{3kT}{m}\right)^{1/2}\frac{1}{n_1}\left[\frac{1}{T}\frac{\partial n_{10}}{\partial z} - \frac{n_{10}}{T^2}\frac{\partial T}{\partial z}\right]\bar{z}_1 \\ &= \left(\frac{3k}{m}\right)\left[\frac{T^{1/2}}{n_{10}}\frac{\partial n_{10}}{\partial z} - \frac{1}{T^{1/2}}\frac{\partial T}{\partial z}\right]\bar{z}_1.\end{aligned} \tag{5.29}$$

Thus the diffusive flux is

$$\begin{aligned}
\bar{c}_1 - \bar{c}_2 =& -\frac{1}{2}(3kT)^{1/2}\left[\frac{1}{\sqrt{m_1}}\left[\frac{T^{1/2}}{n_{10}}\frac{\partial n_{10}}{\partial z} - \frac{1}{T^{1/2}}\frac{\partial T}{\partial z}\right]\bar{z}_1 - \frac{1}{\sqrt{m_2}}\left[\frac{T^{1/2}}{n_{20}}\frac{\partial n_{20}}{\partial z} - \frac{1}{T^{1/2}}\frac{\partial T}{\partial z}\right]\bar{z}_2\right] \\
&-\frac{1}{2}(3kT)^{1/2}\left[+\frac{1}{\sqrt{m_1}}\frac{1}{2T^{1/2}}\frac{\partial T}{\partial z}\bar{z'}_1 - \frac{1}{\sqrt{m_2}}\frac{1}{2T^{1/2}}\frac{\partial T}{\partial z}\right]\bar{z'}_2 \\
=& -\frac{1}{2}(3kT)^{1/2}\left[\left(\frac{\bar{z}_1}{n_{10}\sqrt{m_1}} + \frac{\bar{z}_2}{n_{20}\sqrt{m_2}}\right)\frac{\partial n_{10}}{\partial z} - \left(\frac{\bar{z}_1 - \frac{\bar{z'}_1}{2}}{\sqrt{m_1}} - \frac{\bar{z}_2 - \frac{\bar{z'}_2}{2}}{\sqrt{m_2}}\right)\frac{1}{T}\frac{\partial T}{\partial z}\right] \qquad (5.30) \\
=& -\frac{1}{n_{10}n_{20}}\left[D_{12}\frac{\partial n_{10}}{\partial z} + D_T\frac{1}{T}\frac{\partial T}{\partial z}\right]. \qquad (5.31)
\end{aligned}$$

We integrate over the directions from which molecules approach the plane shows $\bar{z} = \frac{2}{3}l$,where l is mean free path. We now get the Soret coefficient

$$k_T = \frac{\left(l_2 - \frac{l'_2}{2}\sqrt{m_1}\right) - \left(l_1 - \frac{l'_1}{2}\sqrt{m_2}\right)}{l_2\sqrt{m_1}n_{10} + l_1\sqrt{m_2}n_{20}} n_{10}n_{20}. \qquad (5.32)$$

By using the numerical factor $l' = al_1$

$$k_T = \left(1 - \frac{a}{2}\right)\frac{\frac{\sqrt{m_1}}{l_1} - \frac{\sqrt{m_2}}{l_2}}{\frac{n_{10}\sqrt{m_1}}{l_1} + \frac{n_{20}\sqrt{m_2}}{l_2}} n_{10}n_{20}. \qquad (5.33)$$

謝辞

本研究を行うにあたり、終始親切なご指導をいただいた増渕雄一先生、畝山多加志先生、土肥侑也先生、木田拓充先生に御礼申し上げます。他研究室ではあるものの、時間を割いていただき、研究について相談を乗っていただいた田仲由喜夫先生にも御礼申し上げます。また、研究について様々な議論していただいた先輩方や同期に感謝しています。

最後に大学生活を支えてくださった、家族や友人に感謝申し上げます。ありがとうございました。

Bibliography

[1] Noelle Pottier. Nonequilibrium statical physics. 2010.

[2] T.G.Cowling S.Chapman. The mathematical theory of non-uniform gases. 1970.

[3] T.L.IBBS K.E.Grew. Thermal diffusion in gases. 1952.

[4] P J Gardner, D M Heyes, and & S R Preston. *Molecular Physics*, Vol. 73, No. 1, pp. 141–173, 1991.

[5] M. Giglio and A. Vendramini. *Phys. Rev. E*, No. 1.

[6] Rio Kita, Simone Wiegand, and Jutta Luettmer-Strathmann. *J. Chem. Phys*, Vol. 121, p. 3874, 2004.

[7] J. Luettmer-Strathmann. *International Journal of Thermophysics*, Vol. 26, No. 6, pp. 1693–1707, 2005.

[8] B. Rousseau. *EPL*, Vol. 67, , 2004.

[9] Carlos Nieto-Draghi, Josep Bonet Ávalos, and Bernard Rousseau. *The Journal of Chemical Physics*, Vol. 122, p. 3874, 2005.

[10] Simone Wiegand, Forschungszentrum Jülich, Rio Kita, and Hui Ning. 2007.

[11] Sten Sarman and Denis J Evans. Technical Report 4, 1992.

[12] David Macgowan' and Denis J Evans. Technical report, 1986.

[13] R Vogelsang and C Hoheisel. *The Journal of Chemical Physics*, Vol. 89, p. 174503, 1988.

[14] R Vogelsang and C Hoheisel. Technical report, 1988.

[15] R Vogelsang, C Hoheisel, G V Paolini, G Ciccotti, Di Roma, La Sapienza, " Piazzale, and Aldo Moro. Technical report.

[16] Alauddin Ahmed and Richard J Sadus. *Phys.Rev.E.*

[17] Niels Grønbech-Jensen and Oded Farago. *Molecular Physics*, Vol. 111, No. 8, pp. 983–991, 2013.

[18] Dirk Reith, Florian Müller-Plathe, and Florian Mü Ller-Plathe. *The Journal of Chemical Physics*, Vol. 112, p. 8978, 2000.

[19] Peter J.Daivis Billy D.todd. Nonequilibrium molecular dynamics. 2017.

[20] J H Irving and John G Kirkwood. *The Journal of Chemical Physics*, Vol. 18, p. 338, 1950.

[21] Gary Morriss Denis J.Evans. Statistical mechanics of nonequilibrium liquids. 2008.